

# Selective Amplification of a Gravitational Wave Signal Using an Atomic Array

Navdeep Arya<sup>1,2,\*</sup> and Magdalena Zych<sup>1,3,†</sup>

<sup>1</sup>*Department of Physics, Stockholm University, Roslagstullsbacken 21, 106 91 Stockholm, Sweden*

<sup>2</sup>*Department of Physical Sciences, Indian Institute of Science Education & Research (IISER) Mohali, Sector 81 SAS Nagar, Manauli PO 140306 Punjab India*

<sup>3</sup>*ARC Centre for Engineered Quantum Systems, School of Mathematics and Physics, The University of Queensland, St. Lucia, Queensland, 4072, Australia*

We present a novel principle for quantum sensing of gravitational waves by exploiting the collective emission rate of a one-dimensional array of initially uncorrelated atoms to selectively amplify a gravitational wave signal over flat spacetime contributions. In contrast to a single atom, we find that the collective emission rate of the array is sensitive to the gravitational wave at first order in its amplitude. We quantify the collective response of the array to an incident gravitational wave by introducing the notion of the effective number of atoms cooperating to sense the gravitational wave. We determine the optimal interatomic spacing such that the flat spacetime collective effects vanish, but the imprint of the gravitational wave in the emission rate of the array scales nearly quadratically with the number of atoms. The near-quadratic scaling counteracts the small amplitude of the gravitational wave. Furthermore, the coherent photon emission, which encodes the gravitational wave imprint, exhibits well-defined directionality and occurs at frequencies shifted by the wave's frequency. We analyze the setup's response to prototypical gravitational wave signals and show that, for coherent array sizes potentially realizable in the near-term, the two advancements—collective response at first order in the gravitational wave's amplitude, and near-quadratic scaling with the number of atoms—yield a photon emission rate large enough to be resolved by current technology in photon detectors.

## I. INTRODUCTION

A suitably initialized array of atoms in Minkowski (flat) spacetime with sub-wavelength spacing between neighboring atoms can emit light in a delayed, short, and intense burst in a process known as the superradiant decay [1–6]. Details of the decay process sensitively depend on the distribution of atoms and the mode structure of the quantum field to which the atoms are coupled. In samples with linear dimensions much smaller than the atom's transition wavelength, the maximum intensity scales quadratically with the total number of excited atoms [1]. However, in extended samples the scaling parameter is  $\mu N$ , where the 'shape factor'  $\mu$  contains information about the distribution of atoms in the sample and the mode structure of the quantum field to which the atoms are coupled. The  $\mu N$  can be interpreted as the effective number of cooperating atoms [2, 3].

In this work, we investigate the dynamics of a one-dimensional (1D) array of  $N$  identical two-level atoms coupled to a real massless scalar field which in turn is quantized on a plane linearized gravitational wave (GW) background spacetime. Modeling atom-light interactions as atoms linearly coupled to a real massless scalar field is known to capture essential features [7]. A plane GW of frequency  $\omega$ , polarization  $+$  and amplitude  $h_+$  is assumed to propagate transverse to the array of atoms (see Fig. 2). The GW affects the array in two distinct ways. First, by altering the proper distance between the atoms,

this effect scales linearly with the total length of the array or, equivalently, for a given interatomic spacing, the total number of atoms in the array. The second effect comes through the quantum field to which the atoms are coupled and which in turn has been quantized on the GW-background spacetime—the presence of a GW leads to a change in the mode structure of the field. The first effect forms the basis of a large class of GW detection schemes [8–12]. In this work, we investigate the second effect in a 1D array of identical two-level atoms. We show that, in contrast to the first effect, the imprint of the GW in the emission rate of the array can scale *nearly quadratically* with the total number of participating atoms and has a number of features which make this scheme promising for experimental implementation. Since the advantages of the scheme presented here arise from collective quantum effects in atoms interacting with a quantum field on a GW background, our results can more broadly be interpreted as predicting new effects arising at the interface of quantum and general relativistic physics—a research area of growing interest for both theoretical and experimental physics communities [13–17]. The key results established in this work can be summarized as follows:

1. The radiative dynamics of an atomic array coupled to a quantum field in a GW background has three contributions: (a) flat-spacetime (Minkowskian) incoherent emission, (b) Minkowskian collective emission, and (c) GW-dependent collective emission.
2. The collective emission is sensitive to the GW at first order in the GW amplitude. This boosts the

\* navdeep.arya@fysik.su.se

† magdalena.zych@fysik.su.se

signal compared to independent atoms, which respond to the GW only at second order or higher in the already minuscule GW amplitude.

3. The GW-dependent collective emission involves coherent photon emission with well-defined directionality and at frequencies shifted from the atom's transition frequency  $\omega_0$  by the the frequency  $\omega$  of the GW, giving signals at frequencies  $|\omega_0 \pm \omega|$ .
4. The interatomic spacing that maximizes the GW-dependent collective emission, minimizes the Minkowskian collective emission—allowing for “*selective amplification*” of the GW signal.
5. The GW-imprint in the emission rate of the array scales nearly-quadratically with the number of participating atoms as long as the number of atoms in the array is less than an upper limit. The near-quadratic scaling counteracts the smallness of the GW amplitude.

Below, we elaborate on these key findings before presenting details in the subsequent sections:

- (A) The three contributions to the radiative response of the array are:
- (i) *Incoherent Minkowskian emission*: stemming from each atom behaving independently of the others. This process involves incoherent photon emission at the atom's transition frequency  $\omega_0$ . Notably, the transition rates of each individual atom are insensitive to the GW to first order in the GW amplitude. The leading-order effect of a GW on the transition rates of an atom scales as  $h_+^2$  [18–22]. Given that the amplitude of the GWs received on earth is minuscule ( $h_+ \sim 10^{-21} - 10^{-16}$ ), this has discouraged any thought of using radiative processes in atoms to sense GWs.
  - (ii) *Collective Minkowskian emission*: This contribution arises due to the collective behavior of the atoms but is insensitive to the presence of the GW. This process involves coherent photon emission at frequency  $\omega_0$ . This component underlies the conventional (Minkowskian) quantum optical superradiance and may lead to a superradiant burst. In one-dimensional arrays, the superradiant burst survives only for interatomic separations  $d \lesssim 0.25\lambda_0$  (see Fig. 1(a) and refs. [5, 6]), where  $d$  is the interatomic distance and  $\lambda_0$  is the transition wavelength of each atom.
  - (iii) *Collective emission due to the GW*: This contribution stems from collective behavior of the atoms and is sensitive to the incident GW at first order in  $h_+$ . This component of the atomic array's radiative dynamics involves coherent photon emission at frequencies  $|\omega_0 \pm \omega|$ , and is the signal of interest to us.

To summarize the above points, the collective emission of the array is sensitive to the gravitational wave at first order in gravitational wave amplitude. Further, the collective emission due to the GW involves coherent photon emission at frequencies  $|\omega_0 \pm \omega|$ . In contrast, as noted above, the two Minkowskian decay channels involve photon emission at frequency  $\omega_0$ .

- (B) The condition for the collective response of the atoms is different in the presence of a GW. In particular, for an atomic array with  $d/\lambda_0 = 1$ , the collective Minkowskian emission vanishes. In contrast, this configuration of the array is the most suitable for sensing the GW as the *Effective Number of Atoms Cooperating to Sense the GW* scales linearly with the total number of participating atoms up to an upper limit. Consequently, the signature of the GW in the decay rate of the array scales nearly quadratically with the number of atoms. The maximum effective number of atoms cooperating to sense the GW depends on  $\bar{\omega} \equiv \omega/\omega_0$  and the length of the array, as analyzed in Figs. 5(a)-5(c). Additionally, as the radiative response of the array to the incident GW originates from the collective behavior of the atoms, it has a well-defined directionality. As shown in Fig. 3(b), the photons carrying GW-imprint are emitted preferentially along the array.

This paper is organized as follows. In Sec. II, we introduce the setup, superradiant master equation, and the quantization of a massless real scalar field on a classical linearized plane GW-background spacetime. Sec. III discusses the radiative dynamics of the atomic array and presents the results mentioned above. We conclude in Sec. IV with a discussion of possible implementations and an outlook for the results presented.

## II. SETUP

### A. Superradiant Master Equation

As depicted in Fig. 2, consider a one-dimensional array of  $N$  identical two-level atoms each having a monopole moment  $\hat{\mathbf{m}} = (i/2)(\hat{\sigma}_i^- - \hat{\sigma}_i^+)$ , where  $\hat{\sigma}_i^\pm \equiv (\hat{\sigma}_i^x \pm i\hat{\sigma}_i^y)/2$  are the atomic raising and lowering operators with  $\hat{\sigma}_i^x$  and  $\hat{\sigma}_i^y$  being the Pauli  $x$ - and  $y$ -matrices for the  $i$ th atom. The atoms couple to a real massless quantum scalar field  $\hat{\Phi}(\tilde{x})$  through an interaction Hamiltonian given as

$$\hat{H}_I = g \sum_i \hat{\mathbf{m}}_i(t) \hat{\Phi}(t, \mathbf{r}_i), \quad (1)$$

where the sum is over the atoms,  $\mathbf{r}_i$  is the position of  $i$ th atom, and  $g$  is a coupling constant assumed to be small [4, 23]. This interaction Hamiltonian is known to be a good model of atom-light interaction when no exchange of angular momentum is involved [7]. In addition,

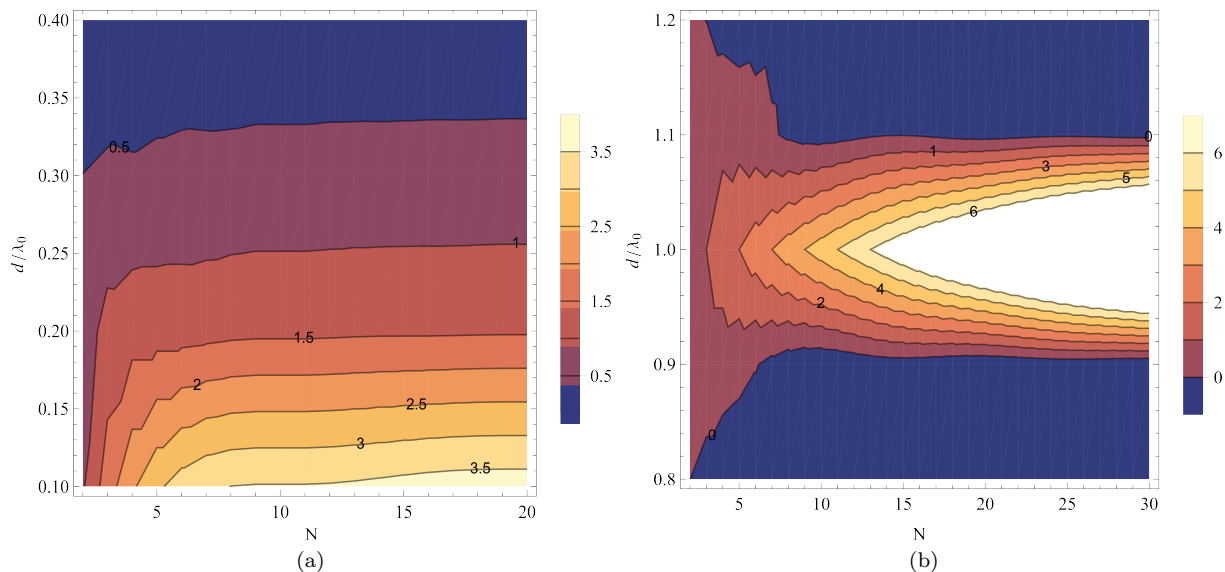


FIG. 1. For extended samples, the collective behavior crucially depends on the distribution of atoms and is governed by what may be called the *shape factor*, denoted as  $\mu$  [see Eq. (18)]. The quantity  $|\mu|N$  can be interpreted as the effective number of cooperating atoms. In a sufficiently small sample, all  $N$  atoms may cooperate, leading to a maximum emission rate scaling as  $N^2$ . In an extended sample, however, the scaling parameter is  $\mu N$ . For atoms coupled to a field quantized on a GW-background spacetime,  $\mu N$  can be decomposed into a Minkowskian contribution  $\mu_M N$  and a contribution  $\mu_{GW} N$  that is sensitive to the GW. **Left Panel.** Contour plot showing constant values of  $\mu_M N$  as a function of the number of atoms  $N$  and  $d/\lambda_0$ , where  $d$  is the lattice constant of a one-dimensional array of identical two-level atoms and  $\lambda_0$  is the transition wavelength of each atom. For an array of atoms to show a superradiant burst,  $\mu_M N$  must be greater than one. Thus, from the contour plot one notes that in Minkowski spacetime a superradiant burst survives for atom spacing  $d \lesssim 0.25\lambda_0$ . **Right Panel.** Contour plot for  $\mu_{GW} N/h_+$ . We can similarly interpret  $\eta \equiv |\mu_{GW} N/h_+$  as the *effective number of atoms cooperating to sense the GW*. From the contour plot, we note that large values of  $\eta$  can be achieved with an atomic array having  $d \approx \lambda_0$ , where the Minkowskian contribution to collective response is highly suppressed.

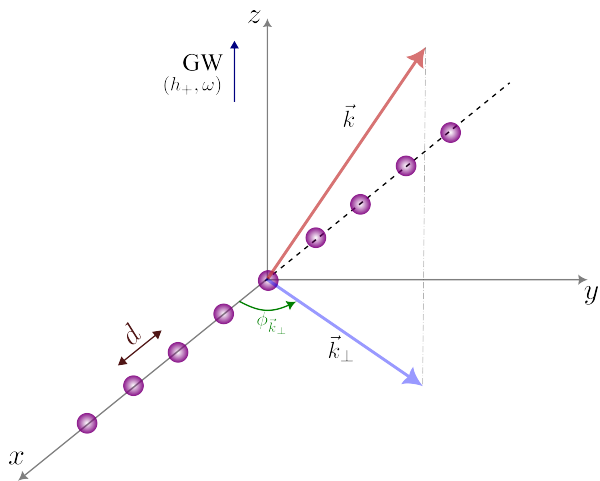


FIG. 2. The setup consists of identical two-level atoms arranged in a one-dimensional array with interatomic distance  $d$  along  $\hat{x}$ -direction. A plane linearized gravitational wave having amplitude  $h_+$ , and frequency  $\omega$  propagates along the  $\hat{z}$ -direction. The subscript ‘+’ denotes the polarization of the gravitational wave. A general field wavevector is denoted by  $\vec{k}$  whereas its projection in the  $xy$ -plane is denoted by  $\vec{k}_\perp$ .

the pointlike interaction Hamiltonian prescription is covariant—leading to transition probabilities invariant under arbitrary diffeomorphisms [24, 25]. The free Hamiltonian of each atom is  $\hat{H}_j = \omega_0 \hat{\sigma}_i^z / 2$ , where  $\hat{\sigma}_i^z$  is the Pauli  $z$ -matrix for the  $i$ th atom. For this system, the superradiant master equation takes the form [4]

$$\begin{aligned} \frac{d\hat{\rho}(t)}{dt} = & -i \left[ \sum_j \hat{H}_j, \hat{\rho}(t) \right] - \frac{ig^2}{2} \sum_{i,j} \int_0^t ds W(\tilde{x}_i, \tilde{x}_j) \\ & \times \left\{ (\hat{m}_i \hat{\sigma}_j^- \hat{\rho}(t) - \hat{\sigma}_j^- \hat{\rho}(t) \hat{m}_i) e^{i\omega_0 s} \right. \\ & \left. - (\hat{m}_i \hat{\sigma}_j^+ \hat{\rho}(t) - \hat{\sigma}_j^+ \hat{\rho}(t) \hat{m}_i) e^{-i\omega_0 s} \right\} \\ & + \text{h.c. of the integrals,} \end{aligned} \quad (2)$$

where  $\hat{\rho}(t)$  is the density operator of the atomic system,  $W(\tilde{x}_i, \tilde{x}_j) \equiv \langle 0 | \hat{\Phi}(t, \mathbf{r}_i) \hat{\Phi}(t-s, \mathbf{r}_j) | 0 \rangle$  is the two-point Wightman function of the field, and ‘h.c.’ denotes hermitian conjugate

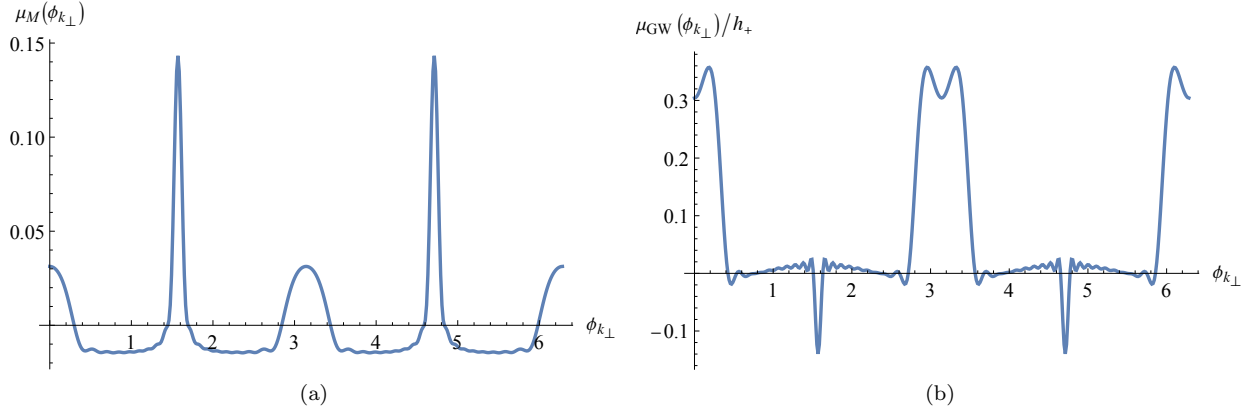


FIG. 3. Comparison of functions  $\mu_M(\phi_{\mathbf{k}_\perp})$  and  $\mu_{\text{GW}}(\phi_{\mathbf{k}_\perp})$  which govern the angular distribution of photons emitted collectively through the Minkowskian and gravitational channels, respectively, by an atomic array with  $d/\lambda_0 = 1$  [see Eq. (F1)]. Referring to the discussion following Eq. (10), and Eq. (19),  $\mu_M = \int_0^{2\pi} d\phi_{\mathbf{k}_\perp} \mu_M(\phi_{\mathbf{k}_\perp}) = 0$  for such an array. Positive values of either quantity mean that the corresponding channel enhances number of photons emitted in that direction by contributing collectively emitted photons, adding to the photons emitted through incoherent Minkowskian decay. Negative values of either quantity mean suppression of incoherently emitted photons in that direction. Note the abundance of photons emitted via the GW channel, having shifted frequencies  $|\omega_0 \pm \omega|$ , along the atomic array, i.e. for  $\phi_{\mathbf{k}_\perp} \approx 0, \pi$ . The plots are for  $N = 10$ . See Appendix F for more details.

### B. Scalar Field Quantized on a GW-background Spacetime

From Eq. (2), we note that the dynamics of the array is controlled by the two-point Wightman function of

the field. For a real massless scalar field quantized on a (classical) linearized plane GW-background spacetime, the Wightman function up to first order in  $h_+$  is obtained in the light-cone coordinates  $u = t - z, v = t + z$  as (see Appendix A) [18, 19]

$$\begin{aligned}
 W(\tilde{x}_i, \tilde{x}'_j) &= \langle 0 | \hat{\Phi}(\tilde{x}_i) \hat{\Phi}(\tilde{x}'_j) | 0 \rangle = \frac{1}{2(2\pi)^3} \int d^2 k_a \int \frac{dk_v}{k_v} \exp\left(-\frac{i}{4k_v}(k_x^2 + k_y^2)\Delta u_{ij}\right) e^{ik_a \Delta r_{ij}^a - ik_v \Delta v_{ij}} \\
 &+ \frac{ih_+}{4(2\pi)^3 \omega} \int d^2 k_a \int \frac{dk_v}{k_v^2} \exp\left(-\frac{i}{4k_v}(k_x^2 + k_y^2)\Delta u_{ij}\right) e^{ik_a \Delta r_{ij}^a - ik_v \Delta v_{ij}} (k_x^2 - k_y^2) \cos\left(\omega \frac{u_i + u'_j}{2}\right) \sin\left(\omega \frac{\Delta u_{ij}}{2}\right) \\
 &\equiv W_M(\tilde{x}_i, \tilde{x}'_j) + W_{\text{GW}}(\tilde{x}_i, \tilde{x}'_j),
 \end{aligned} \tag{3}$$

where  $\tilde{x}$  denotes a spacetime event,  $a \in \{x, y\}$ ,  $\Delta r_{ij}^a$  is the separation between the  $i$ th and  $j$ th atoms in the  $xy$ -plane, and  $W_M(\tilde{x}_i, \tilde{x}'_j)$  and  $W_{\text{GW}}(\tilde{x}_i, \tilde{x}'_j)$  are, respectively, the Minkowski and gravitational wave contributions to the Wightman function up to first order in  $h_+$ .

We are interested in the response of an atomic array arranged transverse to the direction of propagation of the GW. In this connection, we already note a crucial modification in the contribution of transverse field modes  $\mathbf{k}_\perp$  to the response of the array due to presence of the gravitational wave. To this end, we perform the transverse angular integration in the Minkowskian and GW contributions to the Wightman function by writing  $d^2 k_a = dk_\perp k_\perp d\phi_{\mathbf{k}_\perp}$ ,  $k_x = k_\perp \cos \phi_{\mathbf{k}_\perp}$ , and  $k_y = k_\perp \sin \phi_{\mathbf{k}_\perp}$ . The  $\phi_{\mathbf{k}_\perp}$ -integral in  $W_M(\tilde{x}_i, \tilde{x}'_j)$  evaluates to: (a)  $2\pi J_0(\sqrt{2}lk_\perp)$  for  $\Delta x_{ij} = \Delta y_{ij} = l$ , and (b)  $2\pi J_0(lk_\perp)$

for either  $\Delta x_{ij} = l, \Delta y_{ij} = 0$  or  $\Delta x_{ij} = 0, \Delta y_{ij} = l$ . Further, the  $\phi_{\mathbf{k}_\perp}$ -integral in  $W_{\text{GW}}(\tilde{x}_i, \tilde{x}'_j)$  vanishes for  $\Delta x_{ij} = \Delta y_{ij}$  but evaluates to: (a)  $-2\pi J_2(lk_\perp)$  for  $\Delta x_{ij} = l, \Delta y_{ij} = 0$  and (b)  $2\pi J_2(lk_\perp)$  for  $\Delta x_{ij} = 0, \Delta y_{ij} = l$ .

Thus, we learn that the contribution of transverse field modes  $k_\perp$  to the response of the atoms in a 1D array along  $\hat{x}$ -direction in the Minkowski space is governed by  $J_0(k_\perp \Delta x_{ij})$ , but in the presence of a GW the contribution sensitive to the GW is governed by  $J_2(k_\perp \Delta x_{ij})$ . We now exploit this distinction to gain a better control over the contributions of  $W_M(\tilde{x}_i, \tilde{x}'_j)$  and  $W_{\text{GW}}(\tilde{x}_i, \tilde{x}'_j)$  to the radiative response of the array.

### III. RESULTS

#### A. Minkowskian and GW Contributions to the Superradiant Master Equation

For the light-cone coordinates  $u \equiv t - z$  and  $v \equiv t + z$ , we have  $\Delta u_{ij} = t_i - z_i - t_j + z_j$  and  $\Delta v_{ij} = t_i + z_i - t_j - z_j$ . However, we consider an array of atoms in the  $xy$ -plane, that is, in the plane transverse to GW propagation direction. Therefore,  $z$ -coordinate of all the atoms is the same. Thus,  $\Delta u_{ij} = t_i - t_j$  and  $\Delta v_{ij} = t_i - t_j$ . For  $t_i = t, t_j = t - s$ , we get  $\Delta u_{ij} = s, \Delta v_{ij} = s$ , and  $u_i + u_j = 2t - s$ . Further, as noted in the previous section, since GW contribution to Wightman function vanishes for any pair of atoms for which  $\Delta x_{ij} = \Delta y_{ij}$ , we assume that the atoms are separated only along the  $\hat{x}$ -direction.

Using Eqs. (2) and (3), for the Minkowskian contribution to the dissipative dynamics of the array we obtain (see Appendices B and D)

$$\left[ \frac{d\hat{\rho}(t)}{dt} \right]_{\text{M,DD}} = \gamma_0 \sum_{i,j} \frac{\sin(\omega_0 \Delta x_{ij})}{\omega_0 \Delta x_{ij}} \times \left( -\frac{1}{2} \{ \hat{\sigma}_i^+ \hat{\sigma}_j^-, \hat{\rho}(t) \} + \hat{\sigma}_j^- \hat{\rho}(t) \hat{\sigma}_i^+ \right), \quad (4)$$

where  $\gamma_0 \equiv g^2 \omega_0 / 8\pi$  is the spontaneous emission rate of a single atom in Minkowski spacetime, and the subscripts 'M' and 'DD' refer to 'Minkowskian' and 'dissipative dynamics', respectively. Next, by making a change of integration variables in Eq. (3) from  $(k_\perp, k_v)$  to  $(k_\perp, k)$  through the transformations [26]

$$k \equiv k_v + \frac{k_\perp^2}{4k_v}, k_z \equiv k_v - \frac{k_\perp^2}{4k_v}, \quad (5)$$

the leading order GW contribution to the dissipative dynamics of the atomic array, in the  $\omega t \ll 1$  regime, can be written as (see Appendices C and D)

$$\left[ \frac{d\hat{\rho}(t)}{dt} \right]_{\text{GW,DD}}^< = \frac{\pi g^2 h_+}{32(2\pi)^2 \omega} \sum_{i,j} \int_0^\infty dk_\perp k_\perp \times \int_0^\infty dk \frac{2k}{\sqrt{k^2 - k_\perp^2}} \Theta(k - k_\perp) J_2(k_\perp \Delta x_{ij}) \times (\delta(k - \omega_0^+) - \delta(k - \omega_0^-)) (\hat{\sigma}_i^+ \hat{\sigma}_j^- \hat{\rho}(t) - \hat{\sigma}_j^- \hat{\rho}(t) \hat{\sigma}_i^+) + \text{h.c. of the integrals.} \quad (6)$$

Here,  $\Theta(x)$  is the Heaviside theta function,  $\delta(x)$  is the Dirac delta function, and  $\omega_0^\pm \equiv \omega_0 \pm \omega$ . The superscript '<' denotes that this equation is strictly valid only for  $t \ll \omega^{-1}$ .

**Frequency-shifted photons.**— In contrast to the Minkowskian contribution wherein the exchange of energy between the atom and the field is governed by  $\delta(k - \omega_0)$ , the presence of  $\delta(k - \omega_0^\pm)$  in Eq. (6) shows that the evolution of the atomic array attributable to

a GW of frequency  $\omega$  involves photons with frequencies  $|\omega_0 \pm \omega|$ .

Next, evaluating the  $k$  and  $k_\perp$ -integrals in Eq. (6) and incorporating the h.c. terms we obtain

$$\left[ \frac{d\hat{\rho}(t)}{dt} \right]_{\text{GW,DD}}^< = -\frac{\gamma_0 h_+}{8\omega\omega_0} \sum_{i,j} f_{ij}^{\text{GW}}(\omega_0^\pm \Delta x_{ij}) \times \left( -\frac{1}{2} \{ \hat{\sigma}_i^+ \hat{\sigma}_j^-, \hat{\rho}(t) \} + \hat{\sigma}_j^- \hat{\rho}(t) \hat{\sigma}_i^+ \right), \quad (7)$$

where

$$f_{ij}^{\text{GW}}(\omega_0^\pm \Delta x_{ij}) \equiv (\omega_0^+)^2 \tilde{f}_{ij}(\omega_0^+ \Delta x_{ij}) - (\omega_0^-)^2 \tilde{f}_{ij}(\omega_0^- \Delta x_{ij}), \quad (8)$$

with

$$\tilde{f}_{ij}(a\Delta x_{ij}) \equiv (a\Delta x_{ij})^{-2} [4 - 4 \cos(a\Delta x_{ij}) - 2(a\Delta x_{ij}) \sin(a\Delta x_{ij})]. \quad (9)$$

**Functions governing collective behavior in Minkowskian versus GW contributions.**— On comparing Eqs. (4) and (7) we note that the collective behavior of the atoms, sensitive to the GW is governed by a very different function  $f_{ij}^{\text{GW}}(\omega_0^\pm \Delta x_{ij})$ , as compared to the Minkowskian contribution. In the later case, the collective behavior of the atoms is governed by [see Eq. (4)]

$$f_{ij}^{\text{M}}(\omega_0 \Delta x_{ij}) = \frac{\sin(\omega_0 \Delta x_{ij})}{\omega_0 \Delta x_{ij}}. \quad (10)$$

The two functions are compared in Fig. 4. The zeros of

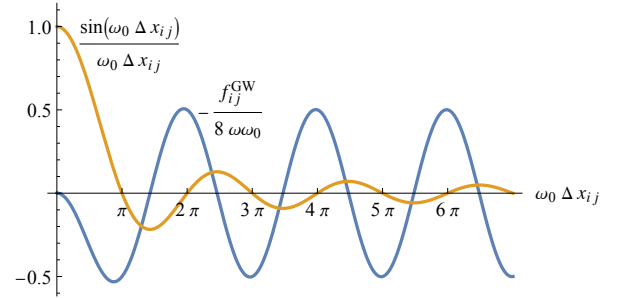


FIG. 4. Comparison of functions governing the collective behavior of atoms. The cooperation among the atoms in Minkowski spacetime is governed by  $\sin(\omega_0 \Delta x_{ij}) / \omega_0 \Delta x_{ij}$ . In contrast, the atomic cooperation *to sense the GW* is governed by  $-f_{ij}^{\text{GW}} / 8\omega\omega_0$ . Refer to Eqs. (13) and (14).

$\sin(\omega_0 \Delta x_{ij}) / \omega_0 \Delta x_{ij}$  occur at  $\omega_0 \Delta x_{ij} = p\pi$ ,  $p \in \mathbb{Z} - \{0\}$ . Therefore, consider the following spatial distribution of  $N$  atoms (let  $N$  be an odd number)

$$x_p = 2\beta \frac{\pi c}{\omega_0} p, p \in \left\{ -\frac{N-1}{2}, \frac{N-1}{2} \right\}; \quad (11)$$



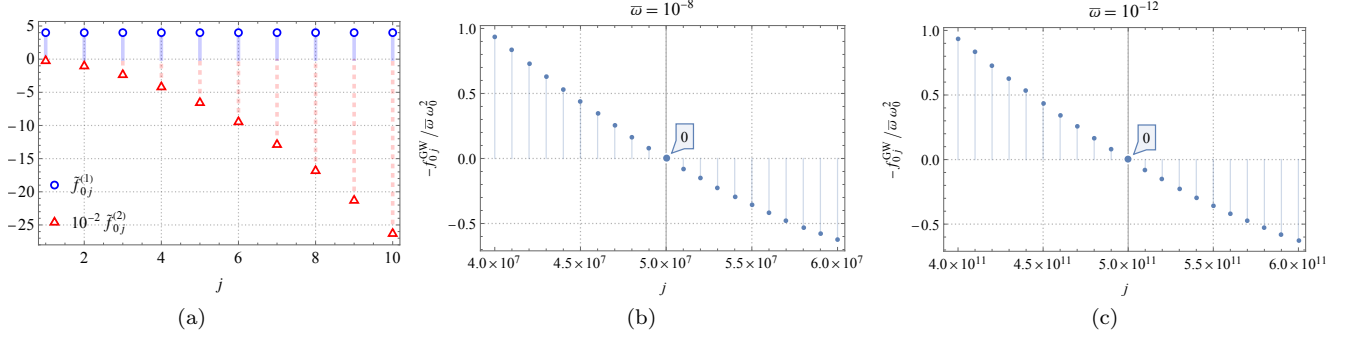


FIG. 5. **Left.** Comparison of  $\tilde{f}_{0j}^{(1)}$  and  $\tilde{f}_{0j}^{(3)}$  as a function of  $j$ . These are the coefficients of  $\bar{\omega}$  and  $\bar{\omega}^3$ , respectively, in the expansion of  $f_{0j}^{\text{GW}}/\omega_0^2$  as a power series in  $\bar{\omega} \equiv \omega/\omega_0$  [refer to Eq. (23)]. The two coefficients are out-of-phase, leading to an upper limit on the effective number of atoms cooperating to sense the GW. **Center and Right.** Plots for  $-f_{0j}^{\text{GW}}/\bar{\omega}\omega_0^2$  as a function of  $j$ . For a given  $\bar{\omega}$  the contribution of  $\tilde{f}_{0j}^{(3)}$  becomes important for a high enough value of  $j$ , and consequently the sign of  $-f_{0j}^{\text{GW}}$  flips. This marks the maximum effective number of atoms,  $\eta_{\text{max}}$ , cooperating to sense the GW. We estimate  $\eta_{\text{max}} \sim 10^7$  and  $10^{11}$  for  $\bar{\omega}$  values of  $10^{-8}$  and  $10^{-12}$ , respectively. All plots are for an array with  $d/\lambda_0 = 1$ . Note that for a given two-level system, the actual number of cooperating atoms can be smaller than the estimate here due to the retardation effects becoming important as the total length  $L$  of the array approaches or exceeds the photon coherence length  $c/\gamma_0$ .

so that we have

$$\omega_0 \Delta x_{ij} = 2\beta(i-j)\pi c. \quad (12)$$

We have introduced the parameter  $\beta$  such that  $\beta = d/\lambda_0$ , where  $d$  is the lattice constant of the atomic array.

### B. Emission Rate of the Atomic Array

Combining Eqs. (4) and (7), we obtain the equation governing the dissipative dynamics of the array in the  $t_{\text{B}} \ll t \ll \omega^{-1}$  regime, where  $t_{\text{B}} \sim L/c$  is the bath correlation time with  $L$  being the total length of the array (see Appendix C):

$$\left[ \frac{d\hat{\rho}(t)}{dt} \right]_{\text{DD}} = \gamma_0 \sum_{i,j} F_{ij} \left( -\frac{1}{2} \{ \hat{\sigma}_i^+ \hat{\sigma}_j^-, \hat{\rho}(t) \} + \hat{\sigma}_j^- \hat{\rho}(t) \hat{\sigma}_i^+ \right), \quad (13)$$

where

$$F_{ij} \equiv f_{ij}^{\text{M}}(\omega_0 \Delta x_{ij}) - \frac{h_+}{8\omega\omega_0} f_{ij}^{\text{GW}}(\omega_0^\pm \Delta x_{ij}). \quad (14)$$

The total emission rate of the array can be obtained from Eq. (13) to be

$$\Gamma_{\downarrow}(t) = \gamma_0 \sum_{i,j} F_{ij} \langle \sigma_i^+ \sigma_j^- \rangle(t). \quad (15)$$

For the initial state of the array, we assume the product state [2, 27]

$$\hat{\rho}(0) = \Pi_i |\theta_0, \varphi_0\rangle_i \langle \theta_0, \varphi_0|, \quad \theta_0 < \pi, \quad (16)$$

where

$$|\theta_0, \varphi_0\rangle_i = \sin(\theta_0/2) e^{-i\varphi_0/2} |e\rangle_i + \cos(\theta_0/2) e^{i\varphi_0/2} |g\rangle_i,$$

with  $|e\rangle$  and  $|g\rangle$  denoting the excited and ground states, respectively, of a two-level atom. With the initial state (16), for the total emission rate of the atomic array we obtain (see Appendix E for details)

$$\begin{aligned} \Gamma_{\downarrow}(t) &= N\gamma_0(\mu N + 1)^2(1 - \cos\theta_0) \\ &\quad \times [(1 + \cos\theta_0)\mu N + 2]e^{\gamma_0 t(\mu N + 1)} \\ &\quad \times \left( [\mu N(1 + \cos\theta_0) + 2]e^{\gamma_0 t(\mu N + 1)} + (1 - \cos\theta_0)\mu N \right)^{-2}, \end{aligned} \quad (17)$$

where the shape factor  $\mu$  is defined as

$$\mu \equiv \frac{1}{N^2} \sum_{i,j;i \neq j} F_{ij}, \quad (18)$$

with  $F_{ij}$  given by Eq. (14). Following the identification of Minkowskian and GW contributions to  $F_{ij}$ , we identify these contributions to  $\mu$  as  $\mu_{\text{M}}$  and  $\mu_{\text{GW}}$ , and write  $\mu = \mu_{\text{M}} + \mu_{\text{GW}}$ . Eq. (17) shows that the atomic array responds to the GW at first order in  $h_+$ .

Since the atom distribution prescribed in Eq. (11) ensures that the Minkowskian cooperation:

$$\mu_{\text{M}} N \equiv \frac{1}{N} \sum_{i,j;i \neq j} f_{ij}^{\text{M}}(\omega_0 \Delta x_{ij}), \quad (19)$$

among the atoms vanishes, we can quantify the effect of the GW on emission rate of the array through the quantity

$$\Delta\Gamma_{\downarrow} \equiv \Gamma_{\downarrow} - \Gamma_{\downarrow}^{\text{inc}}, \quad (20)$$

where  $\Gamma_{\downarrow}^{\text{inc}}$  is the incoherent emission rate of the array and is obtained in the limit  $\mu \rightarrow 0$ :

$$\Gamma_{\downarrow}^{\text{inc}} = \lim_{\mu \rightarrow 0} \Gamma(t) = \frac{1}{2} N(1 - \cos\theta_0) \gamma_0 e^{-\gamma_0 t}. \quad (21)$$

With reference to Eq. (17), one can interpret  $\mu N$  as the *effective number of cooperating atoms* [2, 3]. Similarly, with reference to Eq. (20), the quantity

$$\eta \equiv \frac{\mu_{\text{GW}} N}{h_+} = -\frac{1}{8\omega\omega_0 N} \sum_{i,j;i \neq j} f_{ij}^{\text{GW}}(\omega_0^\pm \Delta x_{ij}), \quad (22)$$

can be interpreted as the *effective number of atoms cooperating to sense the GW*. Equation (20) shows that the strength of the GW's effect imprinted in the array's emission rate depends on the magnitude of  $\mu_{\text{GW}} N/h_+$ .

In the following, we estimate the maximum effective number  $\eta_{\text{max}}$  of the atoms cooperating to sense a GW for two GW signals: one with amplitude  $10^{-21}$  and frequency 100 Hz that lies within the sensitivity window of the Laser Interferometer Gravitational-wave Observatory (LIGO) [28], and a hypothesized high frequency GW signal with amplitude  $10^{-16}$  and MHz frequency [29, 30]. With optical atomic transitions having  $\omega_0 \sim 10^{14}$  Hz, the two signals have  $\bar{\omega} \equiv \omega/\omega_0$  values of  $10^{-12}$  and  $10^{-8}$ , respectively. We then use the  $\eta_{\text{max}}$  estimates to guide us in plotting  $\Delta\Gamma_\downarrow/\gamma_0$  as a function of  $\gamma_0 t$  in Fig. 6 for the two signals for atomic arrays with different number of atoms. Moreover, in Fig. A1 in the Appendices, we compare the  $N$ -scaling of the maxima of  $\Delta\Gamma_\downarrow$  obtained using arrays having  $N < \eta_{\text{max}}$  versus the ones obtained using arrays having  $N > \eta_{\text{max}}$ . We find that the maximum GW-imprint  $\Delta\Gamma_\downarrow^{\text{m}}$  scales nearly-quadratically with the total number of participating atoms as long as the number is less than  $\eta_{\text{max}}$ . However, once  $N$  exceeds  $\eta_{\text{max}}$ , the maximum GW-imprint scales at most linearly with  $N$ .

**Effective Number of Atoms Cooperating to Sense the GW.**—The correlations between  $i$ th and  $j$ th atoms that underlie the pair's sensitivity to the incident GW are captured by  $f_{ij}^{\text{GW}}(\omega_0^\pm \Delta x_{ij})$  and their net total for all the atom pairs determines the effective number  $\mu_{\text{GW}} N/h_+$  of atoms cooperating to sense the GW. The expected cooperation among the atoms can be understood better by looking at the expansion of  $\mu_{\text{GW}}$  as a power series in  $\bar{\omega} \equiv \omega/\omega_0$  for  $\bar{\omega} \ll 1$ . To this end, we obtain

$$\mu_{\text{GW}} N^2 = \frac{h_+}{8\bar{\omega}} \sum_{i,j;i \neq j} \left[ \bar{\omega} \tilde{f}_{ij}^{(1)}(\omega_0 \Delta x_{ij}) + \bar{\omega}^2 \tilde{f}_{ij}^{(2)}(\omega_0 \Delta x_{ij}) + \bar{\omega}^3 \tilde{f}_{ij}^{(3)}(\omega_0 \Delta x_{ij}) + \dots \right], \quad (23)$$

where  $\tilde{f}_{ij}^{(2)}(\omega_0 \Delta x_{ij}) = 0$ ,

$$\tilde{f}_{ij}^{(1)}(\omega_0 \Delta x_{ij}) = 4 \cos(\omega_0 \Delta x_{ij}) - \frac{4 \sin(\omega_0 \Delta x_{ij})}{\omega_0 \Delta x_{ij}}, \quad \text{and} \quad (24a)$$

$$\tilde{f}_{ij}^{(3)}(\omega_0 \Delta x_{ij}) = -\frac{2}{3}(\omega_0 \Delta x_{ij}) \left\{ \sin(\omega_0 \Delta x_{ij}) + \omega_0 \Delta x_{ij} (\cos(\omega_0 \Delta x_{ij})) \right\}. \quad (24b)$$

The components  $\tilde{f}_{ij}^{(1)}(\omega_0 \Delta x_{ij})$  and  $\tilde{f}_{ij}^{(3)}(\omega_0 \Delta x_{ij})$  are plotted in Fig. 5(a), showing that they are out-of-phase. For a given  $\bar{\omega}$  and atom  $i_0$ , beyond a certain  $j$  value  $j_{\text{max}}$ , the contribution of  $\tilde{f}_{ij}^{(3)}(\omega_0 \Delta x_{ij})$  becomes dominant as  $\tilde{f}_{ij}^{(3)}(\omega_0 \Delta x_{ij})$  scales with  $(\Delta x_{ij})^2$ . And since  $\tilde{f}_{ij}^{(1)}$  and  $\tilde{f}_{ij}^{(3)}$  are out-of-phase, this can be interpreted to mean that atoms with  $|j| > |j_{\text{max}}|$  do not cooperate with atom  $i_0$ . We can thus use these observations to estimate  $\eta_{\text{max}}$ , the maximum number of atoms that cooperate to sense the GW. In Figs. 5(b) and 5(c), we plot  $-f_{ij}^{\text{GW}}(\omega_0^\pm \Delta x_{ij})/\bar{\omega}\omega_0^2$  for  $\bar{\omega} = 10^{-8}$  and  $\bar{\omega} = 10^{-12}$  to estimate the corresponding  $\eta_{\text{max}}$  values to be of the order of  $10^7$  and  $10^{11}$ , respectively. The imprint  $\Delta\Gamma_\downarrow$  of an incident GW in the emission rate of an array with the number of excited atoms  $N$  less than the  $\eta_{\text{max}}$  value corresponding to that GW scales nearly-quadratically with  $N$  as depicted in Fig. 6. Once  $N$  exceeds  $\eta_{\text{max}}$ , the sensitivity increases at most linearly if more atoms are added to the array (see Fig. A1 in the Appendices). As the incoherent emission rate of the array also scales linearly with the total number of atoms,  $N = \eta_{\text{max}}$  with  $d = \lambda_0$  sets the optimal size of the array for sensing the GW.

Note that the estimates given above rely on Markovian approximation. Therefore, depending on the choice of  $\lambda_0$  the optimal number of atoms can be smaller than  $\eta_{\text{max}}$  since two atoms separated by more than the photon coherence length  $\sim c/\gamma_0$  are, in general, not expected to behave coherently. For long arrays of atoms, retardation effects can become important and bring in non-Markovian features in the array's dynamics. The retardation and ensuing non-Markovian effects in the 1D array of total length  $L$ , can be quantified in terms of  $\xi = L\gamma_0/c$ , i.e., the total length of the array normalized by the photon coherence length  $c/\gamma_0$  [31]. For the cases depicted in Figs. 6(c) and 6(d),  $\xi$  has the admissible values  $\sim 10^{-2}$  and  $10^{-1}$ , respectively (see [31] for more details). We have also not considered the effect of coherent Hamiltonian dynamics of the atoms in estimating  $\eta_{\text{max}}$  as it introduces only a very slow dephasing in ordered atomic arrays [6]. In fact, in ordered arrays the dominant mechanism responsible for suppression of collective effects has been argued to be the competition between different decay channels available to the atoms [5, 6]. In our case, this effect is accounted for by  $\mu N$ , the effective number of cooperating atoms (see Appendix D).

#### IV. DISCUSSION AND CONCLUSIONS

**Implementation.**— For a GW with amplitude  $h_+ \sim 10^{-21}$  and frequency  $\omega \sim 100$  Hz, one may use the narrow spin-forbidden transition ( $^1S_0 - ^3P_1$ ) in barium-138 having a spontaneous emission rate  $\gamma_0 \sim 25$  kHz and wavelength 791 nm [32]. From Figs. 6(c) and 6(d), we note that the maximum GW-imprint,  $\Delta\Gamma_{\text{max}}^\downarrow$ , is of the order of  $10^{-2}$  Hz and  $5 \times 10^{-1}$  Hz for such atomic arrays having total number of atoms  $N = 10^8$  and  $10^9$ ,

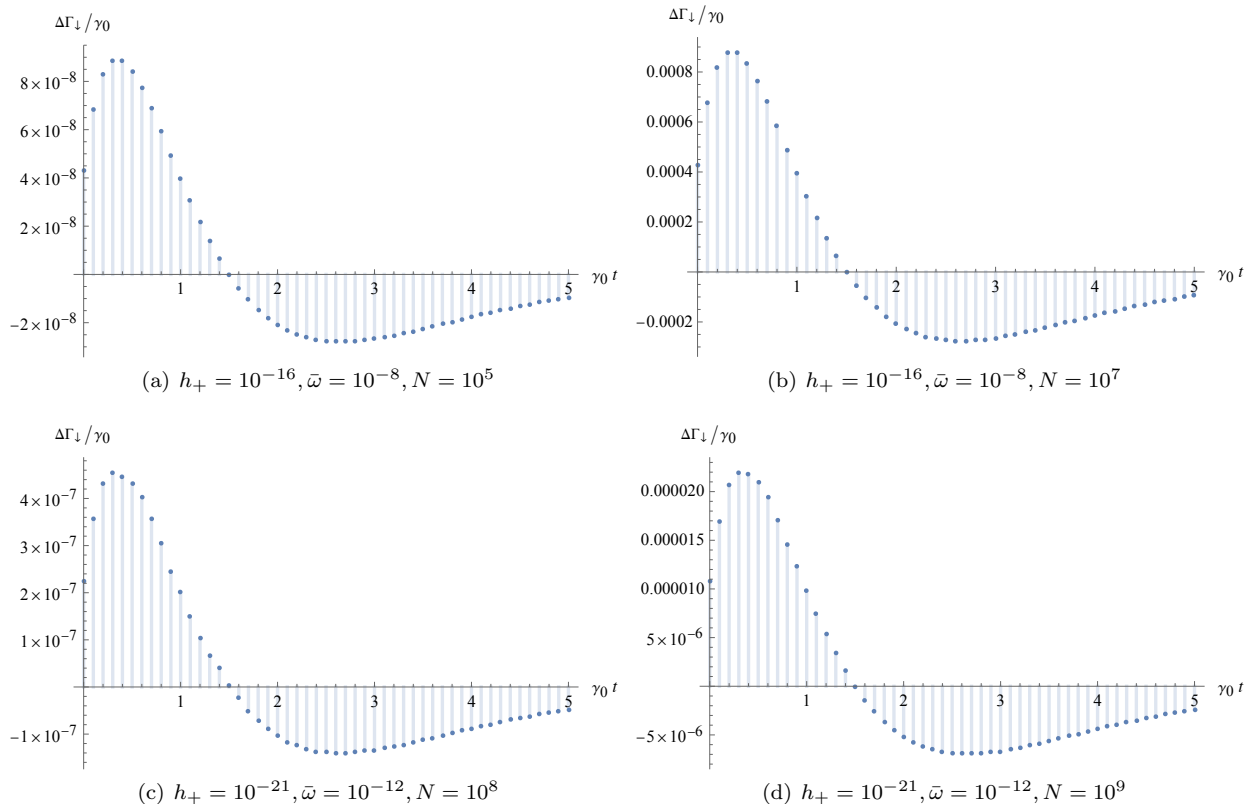


FIG. 6.  $\Delta\Gamma_{\downarrow}/\gamma_0$  versus  $\gamma_0 t$ , where  $\gamma_0$  is the spontaneous decay rate of a single atom. The GW amplitude,  $\bar{\omega}$ , and total number of atoms  $N$  in the array corresponding to each plot are indicated below it. For all the plots,  $N < \eta_{\max}$  and, therefore, the signature of the GW in the decay rate of the array,  $\Delta\Gamma_{\downarrow}$ , scales nearly quadratically with  $N$ . For  $N > \eta_{\max}$  (not shown),  $\Delta\Gamma_{\downarrow}$  scales at most linearly with  $N$  (see Fig. A1). Recall that the incoherent decay rate of array scales linearly with  $N$ . All plots are for an array with  $d/\lambda_0 = 1$  and  $\theta_0 = 0.8\pi$ , which corresponds to 90% excitation of each atom in the array.

respectively. These photon emission rates can be registered with Superconducting Nanowire Single Photon Detectors (SNSPDs), which have been shown, in different experiments, to have near-unity detection efficiency, broad spectral sensitivity, scalability of the detection area, and an ultra-low dark count rate of  $10^{-6}$  Hz [33–37]. In fact, an array with  $N \sim 5 \times 10^6$  would provide a maximum GW-imprint of the order of  $10^{-5}$  Hz, much higher than the dark count rate achievable with SNSPDs. Combined with the distinctive angular distribution of shifted-frequency photons carrying the GW-imprint (see Fig. 3(b)), such an array (having a length  $\sim 4$  m) can already resolve a GW signal of amplitude  $10^{-21}$  and frequency 100 Hz.

From Figs. 6, note that the maxima of  $\Delta\Gamma_{\downarrow}$  occur near  $\gamma_0 t \lesssim 1$ . Therefore, consistent with the fact that we have worked in the  $\omega t \ll 1$  regime, a setup to look for high-frequency GWs in the kHz to MHz range [29] would require working with dipole-allowed atomic transitions. Typical spontaneous emission rates for such transitions are in the range  $10^6$ – $10^9$  Hz. As an illustrative example, the signal strength,  $\Delta\Gamma_{\downarrow}$ , for one such hypothesized GW signal [29, 30] having  $h_+ \sim 10^{-16}$  and  $\omega \sim$  MHz is plotted in Figs. 6(a) and 6(b). For  $N \sim 10^5$ , the imprint of the

GW in the emission rate of the array can get as large as  $10^{-7}\gamma_0$ . Thus, an array of length  $\sim 8$  cm can be expected to provide a detectable signal to test these hypothesized GWs.

Although the signal strengths estimated above are very promising, realization of the required experimental setups is undoubtedly very demanding. Any attempt to design such a setup will have to deal with challenges such as position disorder, partial filling, and inhomogeneous broadening in the atomic array. These effects have been modeled for several platforms [5, 6, 38], and can be quantified in detail depending on a particular implementation, which we leave to future work. Nevertheless, Fig. 1(b) and Fig. 4 show that  $d = \lambda_0$  is not an absolute requirement for the atomic cooperation to sense the GW. Therefore, one can expect small position disorder to not severely hamper the signal. The same can be expected for partial filling as some platforms now allow filling fractions  $\gtrsim 0.9$  [39–42]. The requirement for large coherent atom arrays in our approach overlaps with the needs of quantum information processing applications. The design and development of coherent atom arrays have advanced rapidly over the past decade, with arrays containing more than  $6 \times 10^3$  atoms already demonstrated [47].



*Conclusion.*— We have presented a novel principle for GW sensing leveraging cooperative response of atoms in an array. The Minkowskian cooperation among the atoms can be made to vanish by choosing a suitable lattice constant which is shown to be favorable for the sensing of an incident GW. In other words, the array exhibits cooperative features selectively for the GW contribution to the emission rate.

We demonstrated that in this configuration of the array, the effective number of atoms cooperating to sense the GW scales linearly with the total number of atoms up to an upper bound inherent in the field correlations. Consequently, the imprint of the GW in the radiative dynamics of the array scales nearly quadratically—thus ensuring selective amplification of the incident GW signal. The resulting strong signal demands advanced experimental capabilities but given the rapid advancement in exquisite quantum sensing and control [43–47], to the extent of possibly facilitating single-graviton detection [48], we anticipate the ideas presented here to spark significant interest from the community towards developing this viable novel proposal into a robust scheme for GW sensing.

The scheme can more generally be seen as describing new joint effects arising from quantum theory and general relativity, which is itself an area of growing interest. In fact, the key idea of selective amplification is also expected to facilitate the detection of other much-sought-after but typically very weak effects at the interface of quantum theory and gravity [49]. Furthermore, the ability to selectively amplify the signal of interest will be a valuable addition to quantum metrological tools in general.

## ACKNOWLEDGMENTS

We thank Daniel Braun, Akhil Deswal, Swadheen Dubey, Sandeep K. Goyal, Kinjalk Lochan, Jorma Louko, Jerzy Paczos, Germain Tobar, and Jun Ye for helpful discussions and useful comments. The authors acknowledge funding from Knut and Alice Wallenberg foundation through a Wallenberg Academy Fellowship No. 2021.0119.

## Appendix A: Quantization on a GW-background Spacetime

Assuming that the gravitational field is weak, we can decompose the metric into the flat Minkowski metric  $\eta_{\mu\nu}$  plus a small perturbation  $h_{\mu\nu}$ :

$$g_{\mu\nu} = \eta_{\mu\nu} + h_{\mu\nu}, \quad |h_{\mu\nu}| \ll 1. \quad (\text{A1})$$

The solution of the vacuum linearized Einstein equations in the Transverse-Traceless (TT) gauge leads to the following line element for a plane GW spacetime (with  $z$  as the GW propagation direction) [50]

$$ds^2 = -dt^2 + dz^2 + \{1 + h_+ \cos[\omega(t - z)]\} dx^2 + \{1 - h_+ \cos[\omega(t - z)]\} dy^2 + 2h_\times \cos[\omega(t - z)] dx dy, \quad (\text{A2})$$

where  $h_+$  and  $h_\times$  are the amplitudes of the “plus” and “cross” polarizations, respectively, and  $\omega$  is the frequency of the gravitational wave.

For our analysis we take the background to be a plane gravitational wave (GW) with + polarization. In terms of the light-cone coordinates  $(u, v, x, y)$ , the line element then takes the form

$$ds^2 = -du dv + g_{ab} dx^a dx^b, \quad (\text{A3})$$

where  $a \in \{x, y\}$ ,  $u \equiv t - z$ ,  $v \equiv t + z$ ,  $f(u) \equiv \sqrt{1 + h_+ \cos(\omega u)}$ ,  $g(u) \equiv \sqrt{1 - h_+ \cos(\omega u)}$ , and  $g_{ab} = \text{diag}(f(u)^2, g(u)^2)$ . A complete orthonormal set of the solutions of Klein-Gordon equation in this spacetime is obtained as [51]

$$\phi_{k_v, k_a}(u, v, x, y) = \frac{1}{(2\pi)^{3/2} \sqrt{2k_v}} (\det(g_{ab}(u)))^{-1/4} \exp\left(-\frac{i}{4k_v} \int_0^u du' g^{ab}(u') k_a k_b\right) e^{ik_a x^a - ik_v v}, \quad (\text{A4})$$

where the modes are normalized as  $(\phi_{k_v, k_a}, \phi_{k'_v, k'_a}) = \delta^2(k^a - k'^a) \delta(k_v - k'_v)$ . The integral in Eq. (A4) evaluates to  $\int_0^u du' g^{ab}(u') k_a k_b = (k_x^2 + k_y^2)u - (h_+/\omega)(k_x^2 - k_y^2) \sin(\omega u)$ .

Next, we quantize the field  $\Phi$  by imposing the usual commutation relations between  $\Phi$  and its conjugate momentum  $\pi_\Phi$  and obtain [51]

$$\hat{\Phi}(u, v, x^a) = \int d^2 k_a dk_v \left( \hat{a}_{k_v, k_a} u_{k_v, k_a} + \hat{a}_{k_v, k_a}^\dagger u_{k_v, k_a}^* \right), \quad (\text{A5})$$

with  $[\hat{a}_{k_v, k_a}, \hat{a}_{k'_v, k'_a}^\dagger] = \delta^2(k_a - k'_a) \delta(k_v - k'_v)$ .

*Minkowskian contribution to Wightman function.*— The Wightman function of the scalar field is obtained as given

in Eq. (3). The Minkowskian contribution to the Wightman function is given as

$$W_M(\tilde{x}_i, \tilde{x}'_j) = \frac{1}{2(2\pi)^3} \int_0^\infty dk_\perp k_\perp \int_0^{2\pi} d\phi_{\mathbf{k}_\perp} e^{ik_\perp(\cos\phi_{\mathbf{k}_\perp}\Delta x_{ij} + \sin\phi_{\mathbf{k}_\perp}\Delta y_{ij})} \int \frac{dk_v}{k_v} \exp\left(-\frac{ik_\perp^2}{4k_v}\Delta u_{ij}\right) e^{-ik_v\Delta v_{ij}} \quad (\text{A6})$$

where we have used  $d^2k_a = dk_\perp k_\perp d\phi_{\mathbf{k}_\perp}$ , and  $k_x = k_\perp \cos\phi_{\mathbf{k}_\perp}$ ,  $k_y = k_\perp \sin\phi_{\mathbf{k}_\perp}$ . The  $\phi_{\mathbf{k}_\perp}$ -integral in  $W_M(\tilde{x}_i, \tilde{x}'_j)$  evaluates to: (a)  $2\pi J_0(\sqrt{2}lk_\perp)$  for  $\Delta x_{ij} = \Delta y_{ij} = l$ , and (b)  $2\pi J_0(lk_\perp)$  for either  $\Delta x_{ij} = l, \Delta y_{ij} = 0$  or  $\Delta x_{ij} = 0, \Delta y_{ij} = l$ .

*GW contribution to Wightman function.*— The part of the Wightman function sensitive to the presence of the GW is

$$W_{\text{GW}}(\tilde{x}_i, \tilde{x}'_j) = \frac{ih_+}{4(2\pi)^3\omega} \cos\left(\omega\frac{u_i + u'_j}{2}\right) \sin\left(\omega\frac{\Delta u_{ij}}{2}\right) \int_{-\infty}^\infty d^2k_a (k_x^2 - k_y^2) e^{ik_a\Delta x_{ij}^a} \int_0^\infty \frac{dk_v}{k_v^2} \exp\left(-\frac{ik_\perp^2\Delta u_{ij}}{4k_v}\right) e^{-ik_v\Delta v_{ij}}. \quad (\text{A7})$$

For the integral over transverse field momenta  $k_a$ , we have

$$\int_{-\infty}^\infty d^2k_a (k_x^2 - k_y^2) e^{ik_a\Delta x_{ij}^a} = \int_0^\infty dk_\perp k_\perp^3 \int_0^{2\pi} d\phi_{\mathbf{k}_\perp} (\cos^2\phi_{\mathbf{k}_\perp} - \sin^2\phi_{\mathbf{k}_\perp}) e^{ik_\perp(\cos\phi_{\mathbf{k}_\perp}\Delta x_{ij} + \sin\phi_{\mathbf{k}_\perp}\Delta y_{ij})}. \quad (\text{A8})$$

The  $\phi_{\mathbf{k}_\perp}$ -integral in  $W_{\text{GW}}(\tilde{x}_i, \tilde{x}'_j)$  vanishes for  $\Delta x_{ij} = \Delta y_{ij}$  but evaluates to: (a)  $-2\pi J_2(lk_\perp)$  for  $\Delta x_{ij} = l, \Delta y_{ij} = 0$  and (b)  $2\pi J_2(lk_\perp)$  for  $\Delta x_{ij} = 0, \Delta y_{ij} = l$ .

## Appendix B: Minkowskian contribution to the master equation

Combining Eq. (A6) with the discussion in the paragraph preceding Eq. (4), the Minkowskian contribution to the Wightman function can be written as

$$\langle 0|\hat{\Phi}(t, \mathbf{r}_i)\hat{\Phi}(t-s, \mathbf{r}_j)|0\rangle_M = \frac{1}{2(2\pi)^2} \int_0^\infty dk_\perp k_\perp J_0(k_\perp\Delta x_{ij}) \int \frac{dk_v}{k_v} \exp\left\{-i\left(\frac{k_\perp^2}{4k_v} + k_v\right)s\right\}. \quad (\text{B1})$$

We change the integration variables from  $(k_\perp, k_v)$  to  $(k_\perp, k_z)$  using transformations given in Eq. (5) with  $dk_v dk_\perp/k_v = dk_z dk_\perp/k$ , and a further change of integration variable from  $k_z$  to  $k$  using  $dk_z/k = dk/k_z$  leads to

$$\langle 0|\hat{\Phi}(t, \mathbf{r}_i)\hat{\Phi}(t-s, \mathbf{r}_j)|0\rangle_M = \frac{1}{(2\pi)^2} \int_0^\infty dk_\perp k_\perp J_0(k_\perp\Delta x_{ij}) \int_0^\infty \frac{dk}{k_z} e^{-iks}. \quad (\text{B2})$$

Substituting the expression for the Minkowskian Wightman function in the superradiant master equation (Eq. (2)) and raising the upper limit of the  $s$ -integral to infinity under the Markov approximation, the Minkowskian contribution (marked by subscript M) to the evolution of the density operator of the atomic array is given as

$$\begin{aligned} \left[\frac{d\hat{\rho}(t)}{dt}\right]_M &= -\frac{ig^2}{2(2\pi)^2} \sum_{i,j} \int_0^\infty ds \int_0^\infty dk_\perp k_\perp J_0(k_\perp\Delta x_{ij}) \int_0^\infty dk \frac{\Theta(k-k_\perp)}{\sqrt{k^2-k_\perp^2}} e^{-iks} \\ &\quad \times \left\{ (\hat{\mathbf{m}}_i\hat{\sigma}_j^-\hat{\rho}(t) - \hat{\sigma}_j^-\hat{\rho}(t)\hat{\mathbf{m}}_i) e^{i\omega_0 s} - (\hat{\mathbf{m}}_i\hat{\sigma}_j^+\hat{\rho}(t) - \hat{\sigma}_j^+\hat{\rho}(t)\hat{\mathbf{m}}_i) e^{-i\omega_0 s} \right\} + \text{h.c. of the integrals.} \end{aligned} \quad (\text{B3})$$

The terms coming from  $(\hat{\mathbf{m}}_i\hat{\sigma}_j^+\hat{\rho}(t) - \hat{\sigma}_j^+\hat{\rho}(t)\hat{\mathbf{m}}_i) e^{-i\omega_0 s}$  and  $\text{Im} \int_0^\infty ds \exp\{-i(k-\omega_0)s\}$  in above equation contribute only to the Lamb shift and Van der Waals dipole-dipole interaction among the atoms. We focus on the dissipative dynamics of the atomic array (see Appendix D) and drop these terms to obtain

$$\left[\frac{d\hat{\rho}(t)}{dt}\right]_{\text{M,DD}} = -\frac{ig^2\pi}{2(2\pi)^2} \sum_{i,j} \int_0^\infty dk_\perp k_\perp J_0(k_\perp\Delta x_{ij}) \frac{\Theta(\omega_0-k_\perp)}{\sqrt{\omega_0^2-k_\perp^2}} (\hat{\mathbf{m}}_i\hat{\sigma}_j^-\hat{\rho}(t) - \hat{\sigma}_j^-\hat{\rho}(t)\hat{\mathbf{m}}_i) + \text{h.c.}, \quad (\text{B4})$$

for the Minkowskian contribution to the dissipative dynamics. The subscript DD in  $[d\hat{\rho}(t)/dt]_{\text{M,DD}}$  denotes ‘dissipative dynamics’. Further, evaluating the  $k_\perp$ -integral as

$$\int_0^\infty dk_\perp k_\perp J_0(k_\perp\Delta x_{ij}) \frac{\Theta(\omega_0-k_\perp)}{\sqrt{\omega_0^2-k_\perp^2}} = \frac{\sin(\omega_0\Delta x_{ij})}{\Delta x_{ij}}, \quad (\text{B5})$$

and dropping the fast rotating terms under rotating-wave approximation by replacing  $\hat{\mathbf{m}}_i\hat{\sigma}_j^-\hat{\rho}(t)$  and  $\hat{\sigma}_j^-\hat{\rho}(t)\hat{\mathbf{m}}_i$  by  $(-i/2)\hat{\sigma}_i^+\hat{\sigma}_j^-\hat{\rho}(t)$  and  $(-i/2)\hat{\sigma}_j^-\hat{\rho}(t)\hat{\sigma}_i^+$ , respectively, and incorporating the h.c. terms we obtain

$$\left[\frac{d\hat{\rho}(t)}{dt}\right]_{\text{M,DD}} = \frac{\pi g^2\omega_0}{2(2\pi)^2} \sum_{i,j} \frac{\sin(\omega_0\Delta x_{ij})}{\omega_0\Delta x_{ij}} \left(-\frac{1}{2}\{\hat{\sigma}_i^+\hat{\sigma}_j^-, \hat{\rho}(t)\} + \hat{\sigma}_j^-\hat{\rho}(t)\hat{\sigma}_i^+\right). \quad (\text{B6})$$

### Appendix C: GW contribution to the master equation

From Eqs. (A7) and (A8), the part of the Wightman function sensitive to the presence of the GW can be cast as

$$W_{\text{GW}}(\mathbf{r}_i, \mathbf{s}; \mathbf{r}_j, t-s) = -\frac{h_+}{16(2\pi)^2\omega} [e^{-i\omega t}(e^{i\omega s} - 1) - e^{i\omega t}(e^{-i\omega s} - 1)] \\ \times \int_0^\infty dk_\perp k_\perp^3 \int_0^\infty \frac{dk_v}{k_v^2} \exp\left\{-i\left(\frac{k_\perp^2}{4k_v} + k_v\right)s\right\} J_2(k_\perp \Delta x_{ij}). \quad (\text{C1})$$

Next, we make a change of integration variables from  $(k_\perp, k_v)$  to  $(k_\perp, k)$  in above equation with transformations given in Eq. (5). To this end, we use two different representations of Bessel-K function. First, from the representation [52]

$$K_\nu(xz) = \frac{z^\nu}{2} \int_0^\infty dt t^{-\nu-1} \exp\left[-\frac{x}{2}\left(t + \frac{z^2}{t}\right)\right], \quad (\text{C2})$$

for  $|\arg z| < \pi/4$  or  $|\arg z| = \pi/4$  and  $\text{Re}\{\nu\} < 1$ , we obtain

$$k_\perp K_1(ik_\perp s) = \frac{k_\perp^2}{4} \int_0^\infty \frac{dk_v}{k_v^2} \exp\left[-is\left(k_v + \frac{k_\perp^2}{4k_v}\right)\right]. \quad (\text{C3})$$

From another representation of the Bessel-K [52]:

$$uK_1(u\mu) = \int_u^\infty dx \frac{xe^{-\mu x}}{\sqrt{x^2 - u^2}}, \quad (\text{C4})$$

for  $u > 0, \text{Re}(\mu) > 0$ , we can write

$$k_\perp K_1(ik_\perp s) = \int_{k_\perp}^\infty dk e^{-iks} \frac{k}{\sqrt{k^2 - k_\perp^2}}. \quad (\text{C5})$$

Using representations (C3) and (C5), we achieve the desired transformation and write

$$W_{\text{GW}}(\mathbf{r}_i, t; \mathbf{r}_j, t-s) = -\frac{h_+}{8(2\pi)^2\omega} [e^{-i\omega t}(e^{i\omega s} - 1) - e^{i\omega t}(e^{-i\omega s} - 1)] \\ \times \int_0^\infty dk_\perp k_\perp \int_0^\infty dk \frac{2k}{\sqrt{k^2 - k_\perp^2}} \Theta(k - k_\perp) e^{-iks} J_2(k_\perp \Delta x_{ij}). \quad (\text{C6})$$

Using Eq. (C6) in the superradiant master equation (Eq. (2)), we find that the contribution of the GW to the evolution of the array is governed by (after rotating-wave approximation)

$$\left[\frac{d\hat{\rho}(t)}{dt}\right]_{\text{GW}} = \frac{g^2 h_+}{32(2\pi)^2 \hbar^2 \omega} \sum_{i,j} \int_0^t ds \int_0^\infty dk_\perp k_\perp \int_0^\infty dk \frac{2k}{\sqrt{k^2 - k_\perp^2}} \Theta(k - k_\perp) J_2(k_\perp \Delta x_{ij}) \\ \times \left\{ (\hat{\sigma}_i^+ \hat{\sigma}_j^- \rho(t) - \hat{\sigma}_j^- \rho(t) \hat{\sigma}_i^+) \left[ e^{-i\omega t}(e^{-i(k-\omega_0^+)s} - e^{-i(k-\omega_0)s}) - e^{i\omega t}(e^{-i(k-\omega_0^-)s} - e^{-i(k-\omega_0)s}) \right] \right. \\ \left. + (\hat{\sigma}_i^- \hat{\sigma}_j^+ \rho(t) - \hat{\sigma}_j^+ \rho(t) \hat{\sigma}_i^-) \left[ e^{-i\omega t}(e^{-i(k+\omega_0^-)s} - e^{-i(k+\omega_0)s}) - e^{i\omega t}(e^{-i(k+\omega_0^+)s} - e^{-i(k+\omega_0)s}) \right] \right\} + \text{h.c.} \quad (\text{C7})$$

For an array of total length  $L$ , the bath correlation time  $t_B$  is of the order of  $L/c$ . If the upper limit  $t$  of the  $s$ -integral is already large enough as compared to  $t_B \sim L/c$ , we can safely raise the upper limit of the  $s$ -integral to infinity, this is known as the *Markovian approximation*. Raising the upper limit of the  $s$ -integral to infinity we get an equation that describes the dynamics for  $t \gg t_B$ :

$$\left[\frac{d\hat{\rho}(t)}{dt}\right]_{\text{GW}} = \frac{g^2 h_+}{32(2\pi)^2 \hbar^2 \omega} \sum_{i,j} \int_0^\infty ds \int_0^\infty dk_\perp k_\perp \int_0^\infty dk \frac{2k}{\sqrt{k^2 - k_\perp^2}} \Theta(k - k_\perp) J_2(k_\perp \Delta x_{ij}) \\ \times \left\{ (\hat{\sigma}_i^+ \hat{\sigma}_j^- \rho(t) - \hat{\sigma}_j^- \rho(t) \hat{\sigma}_i^+) \left[ e^{-i\omega t}(e^{-i(k-\omega_0^+)s} - e^{-i(k-\omega_0)s}) - e^{i\omega t}(e^{-i(k-\omega_0^-)s} - e^{-i(k-\omega_0)s}) \right] \right. \\ \left. + (\hat{\sigma}_i^- \hat{\sigma}_j^+ \rho(t) - \hat{\sigma}_j^+ \rho(t) \hat{\sigma}_i^-) \left[ e^{-i\omega t}(e^{-i(k+\omega_0^-)s} - e^{-i(k+\omega_0)s}) - e^{i\omega t}(e^{-i(k+\omega_0^+)s} - e^{-i(k+\omega_0)s}) \right] \right\} + \text{h.c.} \quad (\text{C8})$$

The terms  $(\hat{\sigma}_i^- \hat{\sigma}_j^+ \rho(t) - \hat{\sigma}_j^+ \rho(t) \hat{\sigma}_i^-) e^{-i\omega_0 s}$ ,  $\text{Im} \int_0^\infty ds \exp\{-i(k + \omega_0^\pm)s\}$ , and  $\text{Im} \int_0^\infty ds \exp\{-i(k + \omega_0)s\}$  in above equation contribute only to Lamb shift and Van der Waals dipole-dipole interaction. For now, we focus on the dissipative dynamics of the atomic array (see Appendix D), therefore, dropping these terms and evaluating the  $s$ -integral, we obtain

$$\left[ \frac{d\hat{\rho}(t)}{dt} \right]_{\text{GW,DD}} = \frac{\pi g^2 h_+}{32(2\pi)^2 \hbar^2 \omega} \sum_{i,j} \int_0^\infty dk_\perp k_\perp \int_0^\infty dk \frac{2k}{\sqrt{k^2 - k_\perp^2}} \Theta(k - k_\perp) J_2(k_\perp \Delta x_{ij}) \quad (\text{C9})$$

$$\times \left\{ (\hat{\sigma}_i^+ \hat{\sigma}_j^- \rho(t) - \hat{\sigma}_j^- \rho(t) \hat{\sigma}_i^+) [e^{-i\omega t} (\delta(k - \omega_0^+) - \delta(k - \omega_0)) - e^{i\omega t} (\delta(k - \omega_0^-) - \delta(k - \omega_0))] + \text{h.c.} \right\}$$

**GW contribution in the  $\omega t \ll 1$  regime.**— We now restrict ourselves to time scales such that  $\omega t \ll 1$ , and obtain a master equation that describes the dissipative dynamics in the  $t_B \ll t \ll \omega^{-1}$  regime (marked by superscript ‘<’):

$$\left[ \frac{d\hat{\rho}(t)}{dt} \right]_{\text{GW,DD}}^< = \frac{\pi g^2 h_+}{32(2\pi)^2 \hbar^2 \omega} \sum_{i,j} \int_0^\infty dk_\perp k_\perp \int_0^\infty dk \frac{2k}{\sqrt{k^2 - k_\perp^2}} \Theta(k - k_\perp) J_2(k_\perp \Delta x_{ij}) \quad (\text{C10})$$

$$\times \left\{ (\hat{\sigma}_i^+ \hat{\sigma}_j^- \rho(t) - \hat{\sigma}_j^- \rho(t) \hat{\sigma}_i^+) [(\delta(k - \omega_0^+) - \delta(k - \omega_0)) - (\delta(k - \omega_0^-) - \delta(k - \omega_0))] + \text{h.c.}, \right\}$$

the  $\delta(k - \omega_0)$  terms cancel out, leaving us with

$$\left[ \frac{d\hat{\rho}(t)}{dt} \right]_{\text{GW,DD}}^< = \frac{\pi g^2 h_+}{32(2\pi)^2 \hbar^2 \omega} \sum_{i,j} \int_0^\infty dk_\perp k_\perp \int_0^\infty dk \frac{2k}{\sqrt{k^2 - k_\perp^2}} \Theta(k - k_\perp) J_2(k_\perp \Delta x_{ij}) \quad (\text{C11})$$

$$\times \left\{ (\hat{\sigma}_i^+ \hat{\sigma}_j^- \rho(t) - \hat{\sigma}_j^- \rho(t) \hat{\sigma}_i^+) [\delta(k - \omega_0^+) - \delta(k - \omega_0^-)] + \text{h.c.} \right\}$$

Finally, evaluating the  $k_\perp$ -integral as

$$\int_0^\infty dk_\perp k_\perp \frac{2a}{\sqrt{a^2 - k_\perp^2}} \Theta(a - k_\perp) J_2(k_\perp \Delta x_{ij}) = a^2 \frac{4 - 4 \cos(a \Delta x_{ij}) - 2(a \Delta x_{ij}) \sin(a \Delta x_{ij})}{(a \Delta x_{ij})^2} \quad (\text{C12})$$

and incorporating the h.c. terms we obtain Eq. (7). Thus the total evolution of the density operator  $\hat{\rho}(t)$  is governed by Eq. (13).

#### Appendix D: Dephasing due to coherent dipole-dipole interactions

The coherent Hamiltonian dynamics of the array causes Lamb shift and collective frequency shift for each atom [53]. The inhomogeneity of the collective frequency shift along the array causes a dephasing of the array and can suppress collective effects [4, 6]. From Eq. (B3), one can check that the Minkowskian contribution to the coherent Hamiltonian dynamics is governed by:  $-\gamma_0 \cos(\omega_0 \Delta x_{ij}) / (\omega_0 |\Delta x_{ij}|)$ . Therefore, in contrast to the collective emission rate, the Minkowskian contribution to the collective frequency shifts will not be suppressed for the atom distribution prescribed in Eq. (11). As a result, the dephasing time scale due to coherent dipole-dipole interactions is set by the Minkowskian contribution as the GW contribution is suppressed by the minuscule GW amplitude. As the atoms in the ‘bulk’ of an ordered array experience similar environment, the inhomogeneity of the collective frequency shifts along the array decreases with the total number of atoms in the array. This occurs because the fraction of atoms in the bulk (relative to those on the edges) of the array increases with the total number of atoms [6]. In ordered one-dimensional arrays, the Minkowskian coherent dipole-dipole interaction introduces only a slow dephasing and, in fact, it is the competition between different decay channels that causes a suppression of collective effects in such systems [5, 6]. The number of different decay channels available depends on the lattice constant of the array. In our case, this effect is contained in  $\mu N$ , the effective number of cooperating atoms. As a simplification, we therefore do not delve into the consequences of slow dephasing of the atoms due to coherent dipole-dipole interactions any further in this work, but rather focus on the dissipative dynamics of the array which is expected to decide the fate of collective effects in ordered arrays [5, 6].

#### Appendix E: Emission rate of the atomic array

**Obtaining emission rate from  $d\hat{\rho}/dt$  equation.**— For density operator evolution of the form

$$\frac{d\hat{\rho}(t)}{dt} = \sum_{i,j} K_{ij}(\cdot) \left( -\frac{1}{2} \{ \hat{\sigma}_i^+ \hat{\sigma}_j^-, \hat{\rho}(t) \} + \hat{\sigma}_j^- \hat{\rho}(t) \hat{\sigma}_i^+ \right), \quad (\text{E1})$$

where  $K_{ij}(\cdot)$  is some function of  $\Delta x_{ij}$ , noting that the operator  $\hat{\sigma}_k^+ \hat{\sigma}_k^-$  corresponds to the  $k$ -th atom populating the excited state, the emission rate for the atomic array can be obtained as

$$\Gamma_{\downarrow}(t) = \sum_k \frac{d}{dt} \text{Tr}_A (\hat{\rho}(t) \hat{\sigma}_k^+ \hat{\sigma}_k^-) = \sum_k \text{Tr}_A \left( \frac{d\hat{\rho}(t)}{dt} \hat{\sigma}_k^+ \hat{\sigma}_k^- \right) = \sum_{i,j} K_{ij}(\cdot) \text{Tr}_A \left( \hat{\sigma}_i^+ \hat{\sigma}_j^- \hat{\rho}(t) \right), \quad (\text{E2})$$

where  $\text{Tr}_A$  denotes trace over atoms. Therefore, from Eq. (13) we obtain the total emission rate of the atomic array as

$$\Gamma_{\downarrow}(t) = \Gamma_M(t) + \Gamma_{\text{GW}}^<(t) = \gamma_0 \sum_{i,j} F_{ij} \langle \sigma_i^+ \sigma_j^- \rangle(t), \quad (\text{E3})$$

where  $\langle \sigma_i^+ \sigma_j^- \rangle(t) \equiv \text{Tr}_A (\sigma_i^+ \sigma_j^- \rho(t))$ . To obtain the decay rate as a function of time, we need to evaluate  $\langle \sigma_i^+ \sigma_j^- \rangle(t)$ . We start by noting (suppressing the argument of  $F_{ij}$  for convenience)

$$\sum_{i,j} F_{ij} \langle \sigma_i^+ \sigma_j^- \rangle = \sum_{i,j;i \neq j} F_{ij} \langle \vec{\sigma}_i \cdot \vec{\sigma}_j - \sigma_i^z \sigma_j^z \rangle + \sum_j F_{jj} \langle \sigma_j^+ \sigma_j^- \rangle. \quad (\text{E4})$$

Recalling that the the permutation operator, the operator corresponding to the interchange of  $i$ th and  $j$ th atom, is given by  $P_{ij} = (\mathbb{1} + \vec{\sigma}_i \cdot \vec{\sigma}_j)/2$ , we write

$$\sum_{i,j} F_{ij} \langle \sigma_i^+ \sigma_j^- \rangle = \frac{1}{4} \sum_{i,j;i \neq j} F_{ij} \langle 2P_{ij} - \mathbb{1} \rangle - \frac{1}{4} \sum_{i,j;i \neq j} F_{ij} \langle \sigma_i^z \sigma_j^z \rangle + \sum_j F_{jj} \langle \sigma_j^+ \sigma_j^- \rangle. \quad (\text{E5})$$

At this point, we need to know  $\langle \sigma_i^z \sigma_j^z \rangle$  in order to determine the decay rate of the array. The two-particle mean values  $\langle \sigma_i^z \sigma_j^z \rangle$  involve three-particle mean values and so on [54]. Thus, an exact solution of the problem requires solving an entire hierarchy of equations. To deal with the large  $N$  case, one can introduce appropriate approximations to decouple the multi-particle mean values. For the initial state of the atomic array prescribed in Eq. (16), an appropriate approximation is to assume [2, 27, 54]

$$\langle \sigma_i^z \sigma_j^z \rangle = \langle \sigma_i^z \rangle \langle \sigma_j^z \rangle, \quad (i \neq j). \quad (\text{E6})$$

Note that this approximation does not necessarily imply that the density operator of the atomic array can be written as direct product of density matrices of individual atoms. By decoupling mean values at a higher order, one finds [54] that corrections to Eq. (E6) are of the order  $1/N$ . Therefore, the inaccuracy introduced by approximation (E6) is quite small for large values of  $N$ , the case of interest to us. Under (E6), we obtain

$$\sum_{i,j} F_{ij} \langle \sigma_i^+ \sigma_j^- \rangle = \frac{1}{4} \sum_{i,j;i \neq j} F_{ij} \langle 2P_{ij} - \mathbb{1} \rangle - \frac{1}{4} \sum_{i,j;i \neq j} F_{ij} \langle \sigma_i^z \rangle \langle \sigma_j^z \rangle + \sum_j \langle \sigma_j^+ \sigma_j^- \rangle. \quad (\text{E7})$$

Also, using  $\sigma_j^+ \sigma_j^- = (\mathbb{1} + \sigma_j^z)/2$ , we obtain

$$\sum_j \langle \sigma_j^+ \sigma_j^- \rangle = \frac{1}{2} \sum_j \langle (\mathbb{1} + \sigma_j^z) \rangle = \frac{1}{2} \left( N + \sum_j \langle \sigma_j^z \rangle \right). \quad (\text{E8})$$

Since  $F_{ij}$  is symmetric under the exchange of  $i$  and  $j$ , the evolution governed by Eq. (13) preserves the permutation symmetry if the atomic array is initialized in a permutationally symmetric state. As  $\langle \sigma_j^z \rangle$  is the same for all atoms then, we can write

$$\begin{aligned} \sum_{i,j} F_{ij} \langle \sigma_i^+ \sigma_j^- \rangle &= \frac{1}{4} \sum_{i,j;i \neq j} F_{ij} \langle 2P_{ij} - \mathbb{1} \rangle - \frac{\langle \sigma_a^z \rangle \langle \sigma_b^z \rangle}{4} \sum_{i,j;i \neq j} F_{ij} + \frac{1}{2} \left( N + \sum_j \langle \sigma_j^z \rangle \right) \\ &= \frac{1}{4} \sum_{i,j;i \neq j} F_{ij} \langle 2P_{ij} - \mathbb{1} \rangle - \frac{\sum_{a=1}^N \langle \sigma_a^z \rangle \sum_{b=1}^N \langle \sigma_b^z \rangle}{4N^2} \sum_{i,j;i \neq j} F_{ij} + \frac{1}{2} \left( N + \sum_j \langle \sigma_j^z \rangle \right) \\ &= \frac{1}{4} \sum_{i,j;i \neq j} F_{ij} \langle 2P_{ij} - \mathbb{1} \rangle - \frac{\left( \sum_{a=1}^N \langle \sigma_a^z \rangle \right)^2}{4N^2} \sum_{i,j;i \neq j} F_{ij} + \frac{1}{2} \left( N + \sum_j \langle \sigma_j^z \rangle \right). \end{aligned} \quad (\text{E9})$$



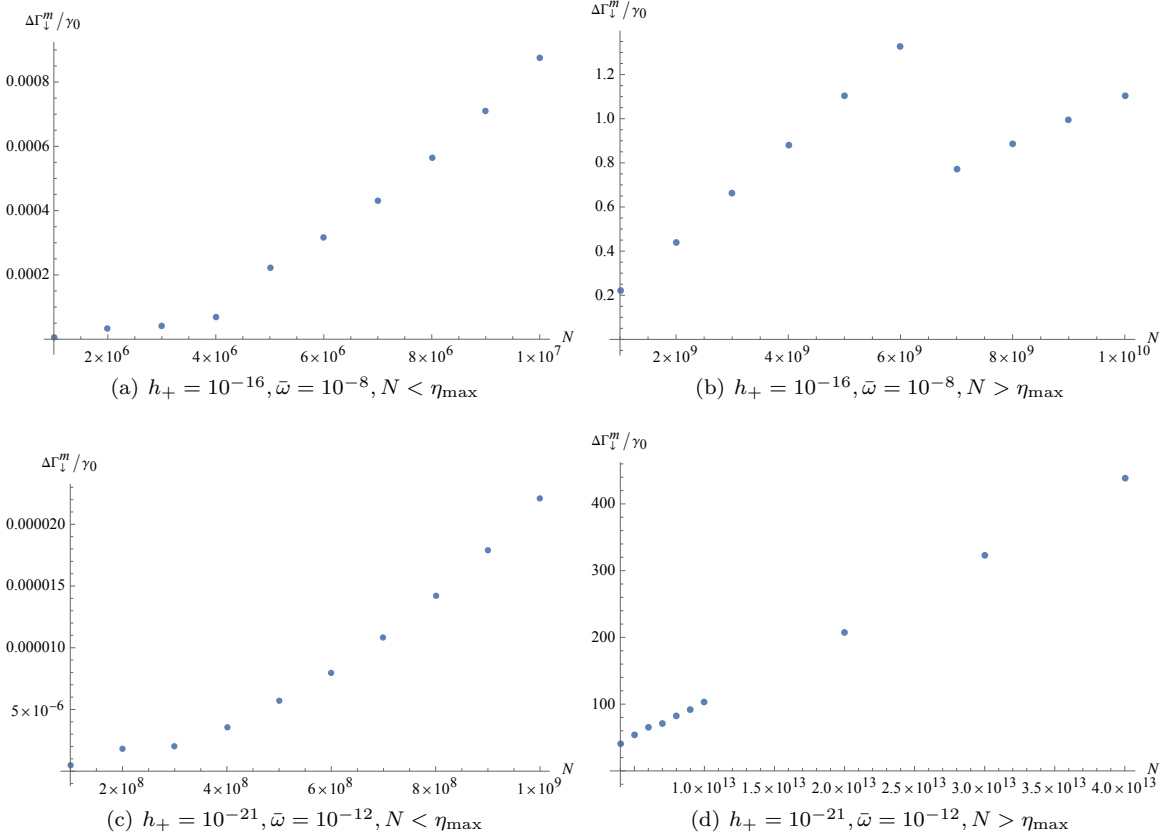


FIG. A1. Scaling of the maxima of (normalized) GW imprint,  $\Delta\Gamma_{\downarrow}^m/\gamma_0$ , in the emission rate of the array as a function of total number of participating atoms  $N$ . **(a,c)** The  $N$  values are less than the  $\eta_{\max}$  value corresponding to each GW signal. Therefore, the imprint of the GW in the emission rate of the array scales nearly quadratically with  $N$ . **(b,d)** For  $N > \eta_{\max}$ ,  $\Delta\Gamma_{\downarrow}^m/\gamma_0$  scales at most linearly with  $N$ . Refer to the discussion in Sec. III B. For all the plots  $\gamma_0 t = 0.3$ ,  $d/\lambda_0 = 1$ , and  $\theta_0 = 0.8\pi$  which corresponds to 90% excitation of each atom in the array.

If the atomic array is initialized in a permutationally symmetric state then  $\langle P_{ij} \rangle = \mathbb{1}$ . Therefore,

$$\sum_{i,j} F_{ij} \langle \sigma_i^+ \sigma_j^- \rangle = \frac{1}{4} \left( 1 - \frac{\left( \sum_{a=1}^N \langle \sigma_a^z \rangle \right)^2}{N^2} \right) \sum_{i,j;i \neq j} F_{ij} + \frac{1}{2} \left( N + \sum_j \langle \sigma_j^z \rangle \right). \quad (\text{E10})$$

In terms of the total (dimensionless) energy of the atomic system:  $W = \frac{1}{2} \sum_{l=1}^N \langle \sigma_l^z \rangle$ , we write

$$\sum_{i,j} F_{ij} \langle \sigma_i^+ \sigma_j^- \rangle = \frac{1}{4} \left( 1 - \frac{4W^2}{N^2} \right) \sum_{i,j;i \neq j} F_{ij} + \frac{1}{2} (N + 2W). \quad (\text{E11})$$

Using Eq. (E3) we obtain a differential equation for  $W(t)$ :

$$\frac{dW}{dt} = \gamma_0 \mu \left( W + \frac{N}{2} \right) \left( W - \frac{N}{2} - \frac{1}{\mu} \right), \quad (\text{E12})$$

where  $\mu$  is as defined in Eq. (18). The initial condition to solve the above equation is determined from Eq. (16) to be  $W(0) = -N \cos \theta_0 / 2$  and the solution is obtained to be

$$W(t) = -\frac{-N[(1 + \cos \theta_0)\mu N + 2]e^{\gamma_0 t(\mu N + 1)} + (1 - \cos \theta_0)N(\mu N + 2)}{-2[(1 + \cos \theta_0)\mu N + 2]e^{\gamma_0 t(\mu N + 1)} - 2(1 - \cos \theta_0)\mu N}, \quad (\text{E13})$$

which gives an emission rate for the array:

$$\Gamma_{\downarrow}(t) = \frac{\gamma_0(1 - \cos \theta_0)N(\mu N + 1)^2[(1 + \cos \theta_0)\mu N + 2]e^{\gamma_0 t(\mu N + 1)}}{([\mu N(1 + \cos \theta_0) + 2]e^{\gamma_0 t(\mu N + 1)} + (1 - \cos \theta_0)\mu N)^2}. \quad (\text{E14})$$

For  $\mu \rightarrow 0$ , we get the incoherent decay rate of the array given as

$$\Gamma_{\downarrow}^{\text{inc}}(t) = \frac{1}{2}N(1 - \cos \theta_0)\gamma_0 e^{-\gamma_0 t}. \quad (\text{E15})$$

### Appendix F: Angular Emission Rate of the Array

From Eq. (E12), we obtain the angular emission rate of the atomic array in the  $xy$ -plane as [2]

$$\Gamma_{\downarrow}(t, \phi_{\mathbf{k}_{\perp}}) = \gamma_0 \left[ \mu(\phi_{\mathbf{k}_{\perp}}) \left( \frac{N^2}{4} - (W(t))^2 \right) + \frac{1}{2\pi} \left( W(t) + \frac{N}{2} \right) \right], \quad (\text{F1})$$

where  $\mu = \int_0^{2\pi} d\phi_{\mathbf{k}_{\perp}} \mu(\phi_{\mathbf{k}_{\perp}})$  and  $\Gamma_{\downarrow}(t) = \int_0^{2\pi} d\phi_{\mathbf{k}_{\perp}} \Gamma_{\downarrow}(t, \phi_{\mathbf{k}_{\perp}})$ . We have already obtained  $W(t)$  in Eq. (E13) and  $\mu(\phi_{\mathbf{k}_{\perp}})$  can be written as  $\mu(\phi_{\mathbf{k}_{\perp}}) = \mu_{\text{M}}(\phi_{\mathbf{k}_{\perp}}) + \mu_{\text{GW}}(\phi_{\mathbf{k}_{\perp}})$ . Below, we determine the Minkowskian and GW contributions to  $\mu(\phi_{\mathbf{k}_{\perp}})$ .

**Minkowski contribution to  $\mu(\phi_{\mathbf{k}_{\perp}})$ .**— The Minkowskian contribution to  $\mu N$  is given by

$$\mu_{\text{M}}N = \frac{1}{N} \sum_{i,j;i \neq j} f_{ij}(\omega_0 \Delta x_{ij}) = \frac{1}{N} \sum_{i,j;i \neq j} \frac{\sin(\omega_0 \Delta x_{ij})}{\Delta x_{ij}} = \frac{1}{N} \sum_{i,j;i \neq j} \int_0^{\infty} dk_{\perp} k_{\perp} J_0(k_{\perp} \Delta x_{ij}) \frac{\Theta(\omega_0 - k_{\perp})}{\sqrt{\omega_0^2 - k_{\perp}^2}}. \quad (\text{F2})$$

Further, using  $\int_0^{2\pi} d\phi_{\mathbf{k}_{\perp}} \exp(ik_{\perp} \Delta x_{ij} \cos \phi_{\mathbf{k}_{\perp}}) = 2\pi J_0(k_{\perp} \Delta x_{ij})$  and writing  $\mu_{\text{M}} = \int_0^{2\pi} d\phi_{\mathbf{k}_{\perp}} \mu_{\text{M}}(\phi_{\mathbf{k}_{\perp}})$  we obtain

$$\mu_{\text{M}}(\phi_{\mathbf{k}_{\perp}}) \equiv \frac{1}{2\pi} \frac{1}{N^2} \sum_{i,j;i \neq j} \int_0^{\infty} dk_{\perp} k_{\perp} e^{ik_{\perp} \Delta x_{ij} \cos \phi_{\mathbf{k}_{\perp}}} \frac{\Theta(\omega_0 - k_{\perp})}{\sqrt{\omega_0^2 - k_{\perp}^2}}. \quad (\text{F3})$$

For the atomic distribution prescribed in Eq. (11), the sum over atoms gives

$$\sum_{i,j;i \neq j} e^{ik_{\perp} \Delta x_{ij} \cos \phi_{\mathbf{k}_{\perp}}} = \sum_{i,j} e^{ik_{\perp} \Delta x_{ij} \cos \phi_{\mathbf{k}_{\perp}}} - N = \frac{\sin^2 \left\{ \frac{\beta N \pi k_{\perp} \cos \phi_{\mathbf{k}_{\perp}}}{\omega_0} \right\}}{\sin^2 \left\{ \frac{\beta \pi k_{\perp} \cos \phi_{\mathbf{k}_{\perp}}}{\omega_0} \right\}} - N \equiv u(\phi_{\mathbf{k}_{\perp}}, k_{\perp}, N, \beta). \quad (\text{F4})$$

Therefore we have

$$\mu_{\text{M}}(\phi_{\mathbf{k}_{\perp}}) \equiv \frac{1}{2\pi N^2} \int_0^{\infty} dk_{\perp} k_{\perp} \frac{\Theta(\omega_0 - k_{\perp})}{\sqrt{\omega_0^2 - k_{\perp}^2}} u(\phi_{\mathbf{k}_{\perp}}, k_{\perp}, N, \beta). \quad (\text{F5})$$

**GW's contribution to  $\mu(\phi_{\mathbf{k}_{\perp}})$ .**— From Eq. (18), we isolate the contribution of the GW as

$$\mu_{\text{GW}}N = -\frac{1}{N} \frac{h_{+}}{8\omega\omega_0} \sum_{i,j;i \neq j} f_{ij}^{\text{GW}}(\omega_0^{\pm} \Delta x_{ij}). \quad (\text{F6})$$

Here  $f_{ij}^{\text{GW}}(\omega_0^{\pm} \Delta x_{ij}) \equiv (\omega_0^{+})^2 \tilde{f}_{ij}(\omega_0^{+} \Delta x_{ij}) - (\omega_0^{-})^2 \tilde{f}_{ij}(\omega_0^{-} \Delta x_{ij})$ , with

$$a^2 \tilde{f}_{ij}(a \Delta x_{ij}) = \int_0^{\infty} dk_{\perp} k_{\perp} f(a, k_{\perp}) J_2(k_{\perp} \Delta x_{ij}) \Theta(a - k_{\perp}); \quad f(a, k_{\perp}) = \frac{2a}{\sqrt{a^2 - k_{\perp}^2}}, \quad (\text{F7})$$

and

$$J_2(k_{\perp} \Delta x_{ij}) = -\frac{1}{2\pi} \int_0^{2\pi} d\phi_{\mathbf{k}_{\perp}} (\cos^2 \phi_{\mathbf{k}_{\perp}} - \sin^2 \phi_{\mathbf{k}_{\perp}}) e^{ik_{\perp} \Delta x_{ij} \cos \phi_{\mathbf{k}_{\perp}}}. \quad (\text{F8})$$

Therefore, for the atomic distribution (11), with the definition  $\mu_{\text{GW}} = \int_0^{2\pi} d\phi_{\mathbf{k}_\perp} \mu_{\text{GW}}(\phi_{\mathbf{k}_\perp})$ , we obtain

$$\mu_{\text{GW}}(\phi_{\mathbf{k}_\perp}) \equiv \frac{h_+}{16\pi\omega\omega_0 N^2} \int_0^\infty dk_\perp k_\perp [f(\omega_0^+, k_\perp)\Theta(\omega_0^+ - k_\perp) - f(\omega_0^-, k_\perp)\Theta(\omega_0^- - k_\perp)] v(\phi_{\mathbf{k}_\perp}, k_\perp, N, \beta), \quad (\text{F9})$$

with

$$v(\phi_{\mathbf{k}_\perp}, k_\perp, N, \beta) \equiv \cos(2\phi_{\mathbf{k}_\perp}) \left[ \frac{\sin^2 \left\{ \frac{\beta N \pi k_\perp \cos \phi_{\mathbf{k}_\perp}}{\omega_0} \right\}}{\sin^2 \left\{ \frac{\beta \pi k_\perp \cos \phi_{\mathbf{k}_\perp}}{\omega_0} \right\}} - N \right]. \quad (\text{F10})$$

**Characteristics of the angular distribution of the emitted photons.**— From Eq. (F1) we note that the angular distribution of the collectively emitted photons is governed by  $\mu(\phi_{\mathbf{k}_\perp}) = \mu_{\text{M}}(\phi_{\mathbf{k}_\perp}) + \mu_{\text{GW}}(\phi_{\mathbf{k}_\perp})$ . In Fig. 3, we have plotted  $\mu_{\text{M}}(\phi_{\mathbf{k}_\perp})$  and  $\mu_{\text{GW}}(\phi_{\mathbf{k}_\perp})/h_+$ . Note the abundance of photons emitted via the GW channel, having shifted frequencies  $|\omega_0 \pm \omega|$ , along the atomic array, i.e. for  $\phi_{\mathbf{k}_\perp} \approx 0, \pi$ .

- 
- [1] R. H. Dicke, Coherence in spontaneous radiation processes, *Phys. Rev.* **93**, 99 (1954).
- [2] N. E. Rehler and J. H. Eberly, Superradiance, *Phys. Rev. A* **3**, 1735 (1971).
- [3] J. H. Eberly, Superradiance Revisited, *American Journal of Physics* **40**, 1374 (1972).
- [4] M. Gross and S. Haroche, Superradiance: An essay on the theory of collective spontaneous emission, *Physics Reports* **93**, 301 (1982).
- [5] S. J. Masson, I. Ferrier-Barbut, L. A. Orozco, A. Browaeys, and A. Asenjo-Garcia, Many-body signatures of collective decay in atomic chains, *Phys. Rev. Lett.* **125**, 263601 (2020).
- [6] S. J. Masson and A. Asenjo-Garcia, Universality of Dicke superradiance in arrays of quantum emitters, *Nature Communications* **13**, 2285 (2022).
- [7] E. Martín-Martínez, M. Montero, and M. del Rey, Wavepacket detection with the Unruh-DeWitt model, *Phys. Rev. D* **87**, 064038 (2013).
- [8] B. P. Abbott, R. Abbott, R. Adhikari, P. Ajith, B. Allen, G. Allen, R. S. Amin, S. B. Anderson, W. G. Anderson, M. A. Arain, *et al.*, LIGO: the laser interferometer gravitational-wave observatory, *Reports on Progress in Physics* **72**, 076901 (2009).
- [9] B. P. Abbott, R. Abbott, T. D. Abbott, M. R. Abernathy, F. Acernese, K. Ackley, C. Adams, T. Adams, P. Addesso, R. X. Adhikari, *et al.* (LIGO Scientific Collaboration and Virgo Collaboration), Observation of gravitational waves from a binary black hole merger, *Phys. Rev. Lett.* **116**, 061102 (2016).
- [10] B. P. Abbott, R. Abbott, T. D. Abbott, M. R. Abernathy, F. Acernese, K. Ackley, C. Adams, T. Adams, P. Addesso, R. X. Adhikari, *et al.* (LIGO Scientific Collaboration and Virgo Collaboration), GW151226: Observation of gravitational waves from a 22-solar-mass binary black hole coalescence, *Phys. Rev. Lett.* **116**, 241103 (2016).
- [11] S. Detweiler, Pulsar timing measurements and the search for gravitational waves, *Astrophys. J.* **234**, 1100 (1979).
- [12] J. W. Armstrong, Low-frequency gravitational wave searches using spacecraft doppler tracking, *Living Reviews in Relativity* **9**, 1 (2006).
- [13] M. Zych, F. Costa, I. Pikovski, and Č. Brukner, Quantum interferometric visibility as a witness of general relativistic proper time, *Nature Communications* **2**, 505 (2011).
- [14] M. A. Hohensee, B. Estey, P. Hamilton, A. Zeilinger, and H. Müller, Force-free gravitational redshift: Proposed gravitational aharonov-bohm experiment, *Phys. Rev. Lett.* **108**, 230404 (2012).
- [15] I. Pikovski, M. Zych, F. Costa, and Č. Brukner, Universal decoherence due to gravitational time dilation, *Nature Physics* **11**, 668 (2015).
- [16] P. Asenbaum, C. Overstreet, T. Kovachy, D. D. Brown, J. M. Hogan, and M. A. Kasevich, Phase shift in an atom interferometer due to spacetime curvature across its wave function, *Phys. Rev. Lett.* **118**, 183602 (2017).
- [17] C. Overstreet, P. Asenbaum, J. Curti, M. Kim, and M. A. Kasevich, Observation of a gravitational aharonov-bohm effect, *Science* **375**, 226 (2022).
- [18] Q. Xu, S. Ali Ahmad, and A. R. H. Smith, Gravitational waves affect vacuum entanglement, *Phys. Rev. D* **102**, 065019 (2020).
- [19] F. Gray, D. Kubizňák, T. May, S. Timmerman, and E. Tjoa, Quantum imprints of gravitational shockwaves, *Journal of High Energy Physics* **2021**, 54 (2021).
- [20] T. Prokopec, Gravitational wave signals in an Unruh-DeWitt detector, *Classical and Quantum Gravity* **40**, 035007 (2023).
- [21] S. Barman, I. Chakraborty, and S. Mukherjee, Entanglement harvesting for different gravitational wave burst profiles with and without memory, *Journal of High Energy Physics* **2023**, 180 (2023).
- [22] S. Barman, I. Chakraborty, and S. Mukherjee, Signatures of gravitational wave memory in the radiative process of entangled quantum probes, arXiv:2405.18277 [10.48550/arXiv.2405.18277](https://arxiv.org/abs/2405.18277) (2024).
- [23] H.-P. Breuer and F. Petruccione, *The theory of open quantum systems* (Oxford University Press on Demand, 2002).
- [24] E. Martín-Martínez, T. R. Perche, and B. de S. L. Torres, General relativistic quantum optics: Finite-size particle detector models in curved spacetimes, *Phys. Rev. D* **101**, 045017 (2020).
- [25] E. Martín-Martínez, T. R. Perche, and B. d. S. L. Torres, Broken covariance of particle detector models in relativistic quantum information, *Phys. Rev. D* **103**, 025007 (2021).

- (2021).
- [26] P. Jones, P. McDougall, and D. Singleton, Particle production in a gravitational wave background, *Phys. Rev. D* **95**, 065010 (2017).
- [27] G. S. Agarwal, Master-equation approach to spontaneous emission, *Phys. Rev. A* **2**, 2038 (1970).
- [28] D. V. Martynov, E. D. Hall, B. P. Abbott, R. Abbott, T. D. Abbott, C. Adams, R. X. Adhikari, *et al.*, Sensitivity of the advanced LIGO detectors at the beginning of gravitational wave astronomy, *Phys. Rev. D* **93**, 112004 (2016).
- [29] M. Goryachev, W. M. Campbell, I. S. Heng, S. Galliou, E. N. Ivanov, and M. E. Tobar, Rare events detected with a bulk acoustic wave high frequency gravitational wave antenna, *Phys. Rev. Lett.* **127**, 071102 (2021).
- [30] N. Aggarwal, O. D. Aguiar, A. Bauswein, G. Cella, S. Clesse, A. M. Cruise, V. Domcke, D. G. Figueroa, A. Geraci, M. Goryachev, H. Grote, M. Hindmarsh, F. Muia, N. Mukund, D. Ottaway, M. Peloso, F. Quevedo, A. Ricciardone, J. Steinlechner, S. Steinlechner, S. Sun, M. E. Tobar, F. Torrenti, C. Ünäl, and G. White, Challenges and opportunities of gravitational-wave searches at MHz to GHz frequencies, *Living Reviews in Relativity* **24**, 4 (2021).
- [31] K. Sinha, P. Meystre, E. A. Goldschmidt, F. K. Fatemi, S. L. Rolston, and P. Solano, Non-markovian collective emission from macroscopically separated emitters, *Phys. Rev. Lett.* **124**, 043603 (2020).
- [32] J. Kim, D. Yang, S. hoon Oh, and K. An, Coherent single-atom superradiance, *Science* **359**, 662 (2018).
- [33] E. E. Wollman, V. B. Verma, A. D. Beyer, R. M. Briggs, B. Korzh, J. P. Allmaras, F. Marsili, A. E. Lita, R. P. Mirin, S. W. Nam, and M. D. Shaw, UV superconducting nanowire single-photon detectors with high efficiency, low noise, and 4 K operating temperature, *Opt. Express* **25**, 26792 (2017).
- [34] Y. Hochberg, I. Charaev, S.-W. Nam, V. Verma, M. Colangelo, and K. K. Berggren, Detecting sub-GeV dark matter with superconducting nanowires, *Phys. Rev. Lett.* **123**, 151802 (2019).
- [35] D. V. Reddy, R. R. Nerem, S. W. Nam, R. P. Mirin, and V. B. Verma, Superconducting nanowire single-photon detectors with 98% system detection efficiency at 1550 nm, *Optica* **7**, 1649 (2020).
- [36] V. B. Verma, B. Korzh, A. B. Walter, A. E. Lita, R. M. Briggs, M. Colangelo, Y. Zhai, E. E. Wollman, A. D. Beyer, J. P. Allmaras, H. Vora, D. Zhu, E. Schmidt, A. G. Kozorezov, K. K. Berggren, R. P. Mirin, S. W. Nam, and M. D. Shaw, Single-photon detection in the mid-infrared up to 10  $\mu\text{m}$  wavelength using tungsten silicide superconducting nanowire detectors, *APL Photonics* **6**, 056101 (2021).
- [37] J. Chiles, I. Charaev, R. Lasenby, M. Baryakhtar, J. Huang, A. Roshko, G. Burton, M. Colangelo, K. Van Tilburg, A. Arvanitaki, S. W. Nam, and K. K. Berggren, New constraints on dark photon dark matter with superconducting nanowire detectors in an optical haloscope, *Phys. Rev. Lett.* **128**, 231802 (2022).
- [38] O. Rubies-Bigorda, S. Ostermann, and S. F. Yelin, Characterizing superradiant dynamics in atomic arrays via a cumulant expansion approach, *Phys. Rev. Res.* **5**, 013091 (2023).
- [39] M. Endres, H. Bernien, A. Keesling, H. Levine, E. R. Anschuetz, A. Krajenbrink, C. Senko, V. Vuletic, M. Greiner, and M. D. Lukin, Atom-by-atom assembly of defect-free one-dimensional cold atom arrays, *Science* **354**, 1024 (2016).
- [40] D. Barredo, S. de Léséleuc, V. Lienhard, T. Lahaye, and A. Browaeys, An atom-by-atom assembler of defect-free arbitrary two-dimensional atomic arrays, *Science* **354**, 1021 (2016).
- [41] D. Barredo, V. Lienhard, S. de Léséleuc, T. Lahaye, and A. Browaeys, Synthetic three-dimensional atomic structures assembled atom by atom, *Nature* **561**, 79 (2018).
- [42] H. Kim, W. Lee, H.-g. Lee, H. Jo, Y. Song, and J. Ahn, In situ single-atom array synthesis using dynamic holographic optical tweezers, *Nature Communications* **7**, 13317 (2016).
- [43] M. A. Norcia, H. Kim, W. B. Cairncross, M. Stone, A. Ryou, M. Jaffe, M. O. Brown, K. Barnes, P. Battaglino, T. C. Bohdanowicz, A. Brown, K. Casella, C.-A. Chen, R. Coxe, D. Crow, J. Epstein, C. Griger, E. Halperin, F. Hummel, A. M. W. Jones, J. M. Kindem, J. King, K. Kotru, J. Lauigan, M. Li, M. Lu, E. Megidish, J. Marjanovic, M. McDonald, T. Mittiga, J. A. Muniz, S. Narayanaswami, C. Nishiguchi, T. Paule, K. A. Pawlak, L. S. Peng, K. L. Pudenz, D. Rodríguez Pérez, A. Smull, D. Stack, M. Urbanek, R. J. M. van de Veerdonk, Z. Vendeiro, L. Wadleigh, T. Wilkason, T.-Y. Wu, X. Xie, E. Zaly-Geller, X. Zhang, and B. J. Bloom, Iterative assembly of  $^{171}\text{Yb}$  atom arrays with cavity-enhanced optical lattices, *PRX Quantum* **5**, 030316 (2024).
- [44] J. Ye and P. Zoller, Essay: Quantum sensing with atomic, molecular, and optical platforms for fundamental physics, *Phys. Rev. Lett.* **132**, 190001 (2024).
- [45] R. Tao, M. Ammenwerth, F. Gyger, I. Bloch, and J. Zeiher, High-fidelity detection of large-scale atom arrays in an optical lattice, *Phys. Rev. Lett.* **133**, 013401 (2024).
- [46] F. Gyger, M. Ammenwerth, R. Tao, H. Timme, S. Snigirev, I. Bloch, and J. Zeiher, Continuous operation of large-scale atom arrays in optical lattices, *Phys. Rev. Res.* **6**, 033104 (2024).
- [47] H. J. Manetsch, G. Nomura, E. Bataille, K. H. Leung, X. Lv, and M. Endres, *A tweezer array with 6100 highly coherent atomic qubits* (2024), [arXiv:2403.12021](https://arxiv.org/abs/2403.12021).
- [48] G. Tobar, S. K. Manikandan, T. Beitel, and I. Pikovskii, Detecting single gravitons with quantum sensing, *Nature Communications* **15**, 7229 (2024).
- [49] R. Howl, L. Hackermüller, D. E. Bruschi, and I. Fuentes, Gravity in the quantum lab, *Advances in Physics: X* **3**, 1383184 (2018).
- [50] M. Maggiore, *Gravitational Waves: Volume 1: Theory and Experiments* (Oxford University Press, 2007).
- [51] J. Garriga and E. Verdaguer, Scattering of quantum particles by gravitational plane waves, *Phys. Rev. D* **43**, 391 (1991).
- [52] A. Jeffrey, D. Zwillinger, I. Gradshteyn, and I. Ryzhik, eds., *Table of Integrals, Series, and Products (Seventh Edition)* (Academic Press, Boston, 2007).
- [53] R. Friedberg, S. Hartmann, and J. Manassah, Frequency shifts in emission and absorption by resonant systems of two-level atoms, *Physics Reports* **7**, 101 (1973).
- [54] G. S. Agarwal, Master-equation approach to spontaneous emission. III. many-body aspects of emission from two-level atoms and the effect of inhomogeneous broadening, *Phys. Rev. A* **4**, 1791 (1971).